VlbZIP30 of grapevine functions in drought tolerance via the abscisic acid core signaling pathway

Mingxing Tu[1,2,*], Xianhang Wang[1,2,*], Yanxun Zhu[1,2], Dejun Wang[1,2], Xuechuan Zhang[3], Ye Cui[3], Yajuan Li[1,2], Min Gao[1,2], Zhi Li[1,2], Xiping Wang[1,2,†]

[1]State Key Laboratory of Crop Stress Biology in Arid Areas, College of Horticulture, Northwest A&F University, Yangling, Shaanxi 712100, China

[2]Key Laboratory of Horticultural Plant Biology and Germplasm Innovation in Northwest China, Ministry of Agriculture, Northwest A&F University, Yangling, Shaanxi 712100, China

[3]Biomarker Technologies Corporation, Beijing 101300, China

* These authors contributed equally to this work.

† Correspondence: wangxiping@nwsuaf.edu.cn

Running title: *VlbZIP30* positively regulate plant drought tolerance

Highlight

VlbZIP30 positively regulate plant drought tolerance through regulated the expression of 27 grapevine candidate genes via G-box *cis*-element (MCACGTGK) in ABA signaling pathway.

Abstract

Drought stress limits the growth and development of grapevines, thereby reducing productivity, but the mechanisms by which grapevines respond to drought stress remain largely uncharacterized. Here, we characterized a group A bZIP gene from 'Kyoho' grapevine, *VlbZIP30*, which was shown to be induced by abscisic acid (ABA) and dehydration stress. Overexpression of *VlbZIP30* in transgenic Arabidopsis enhanced dehydration tolerance during seed germination, and in the seedling and adult stages. Transcriptome analysis revealed that a major proportion of ABA- and/or drought-responsive genes are transcriptionally regulated by *VlbZIP30* during ABA or mannitol treatment at the cotyledon greening stage. We identified an *A. thaliana* G-box motif (CACGTG) and a potential grapevine G-box motif (MCACGTGK) in the promoters of the 39 selected *A. thaliana* genes up-regulated in the transgenic plants and in the 35 grapevine homologs, respectively. Subsequently, using two grapevine-related databases, we found that 74% and 84% (a total of 27 genes) of the detected grapevine genes were significantly up-regulated by ABA and drought stress, respectively, suggesting that these 27 genes involve in ABA or dehydration stress and may be regulated by *VlbZIP30* in grapevine. We propose that *VlbZIP30* functions as a positive regulator of drought-responsive signaling in the ABA core signaling pathway.

Keywords

Grapevine, *VlbZIP30*, Drought stress, ABA, RNA-seq, G-box.

Introduction

Grapevines are amongst the world's major fruit crops, and their fruits can be consumed either fresh or dried or be processed into wines, spirits and vinegar, or transformed into pharmaceutical products that promote human health (Pilati *et al*., 2017). However, abiotic stress, such as drought, perturb the metabolism and growth of grapevines, leading to a loss of yield and reduced fruit quality (Ferreira *et al*., 2004). Consequently, increasing the resistance of grapevines to drought stress is an important factor in ensuring yield stability.

Stress signaling in plants can be transduced by various signaling components, including second messengers (e.g. Ca^{2+}), signal transduction factors, including protein kinases and phosphatases, hormonessuch as abscisic acid (ABA), and transcription factors (TFs). Such signaling associated with drought has been shown to cause changes in physiological, morphological and molecular processes, including the activation of many drought stress-related genes and the accumulation of a range of proteins, reflecting a drought stress response (Zhu, 2002; Yamaguchi-Shinozaki and Shinozaki, 2006; Lata and Prasad, 2011; Tang *et al*., 2012).

ABA is considered to be a stress hormone and has been particularly associated with drought tolerance, although it is also involved in various developmental processes, including seed germination, seedling growth and development (Finkelstein *et al.*, 2002; Tang *et al.*, 2012). In the context of a drought response it has been shown to mediate stomatal closure and to promote cuticular wax biosynthesis (Nambara and Kuchitsu, 2011). Analyses of the underlying molecular mechanisms have demonstrated that both ABA-dependent and ABA-independent pathways are involved in drought stress responses (Shinozaki and Yamaguchi-Shinozaki, 2000; Yamaguchi-Shinozaki and Shinozaki, 2006). ABA-mediated drought tolerance involves complex signaling networks, the core components of which have been identified. Briefly, when ABA is present, it binds to the ABA receptors PYR/PYL/RCAR (PYRABACTIN RESISTANCE1/PYR1-like/REGULATORY COMPONENT OF ABA RECEPTOR1), which interact with the PP2C (PROTEIN

PHOSPHATASE 2C) proteins, forming a complex and releasing the inhibitory effect of PP2Cs on SnRK2 (SUCROSE-NONFERMENTING1-RELATED PROTEIN KINASE2) protein kinases. The activated SnRK2s proteins subsequently phosphorylate different downstream TFs, such as AREB1 (ABA-RESPONSE-ELEMENT BINDING1) and ABI5 (ABA INSENSITIVE5), which regulate the expression of ABA-responsive genes (Fujii and Zhu, 2009; Fujita *et al*., 2009; Ma *et al*., 2009; Nakashima *et al*., 2009; Park *et al*., 2009; Danquah *et al*., 2014).

TFs are generally identified according to conserved sequences, known as the DNA-binding domains. One of the largest TF families in higher plants is the bZIP family, members of which are characterized by a basic region/leucine zipper domain (Van Leene *et al*., 2016). Previous studies have shown that bZIP proteins function as regulators of signaling networks by specifically binding *cis*-elements containing an core ACGT, such as the ABA-responsive element (ABRE; PyACGTGGC), the G-box (CACGTG) and the C-box (GACGTC) (Yamaguchi-Shinozaki *et al*., 1990; Foster *et al*., 1994), in the promoters of their target genes, to either activate or repress their expression (Mitsuda and Ohme-Takagi, 2009).

A number of studies have shown that bZIP TFs are important regulators of drought stress signaling in the ABA-dependent pathway, mostly in association with seed germination and post-germination growth. The involvement of bZIP TFs (*ABF1*, *AREB1/ABF2*, *ABF3*, *AREB2/ABF4*) in the regulation of drought responses was first reported in the model plant *Arabidopsis thaliana* (Kang *et al*., 2002; Kim *et al*., 2004; Fujita *et al*., 2005; Yoshida *et al*., 2010; Yoshida *et al*., 2015). Following these studies, drought-related bZIP genes have been identified in a range of other species, including *OsABI5* in rice (*Oryza sativa*) (Zou *et al*., 2008), *LIP19* in wheat (*Triticumaestivum*) (Kobayashi *et al*., 2008), *ABP9* in maize (*Zea mays*) (Zhang *et al*., 2011), *SlAREB1* in tomato (*Solanum lycopersicum*) (Orellana *et al*., 2010), *GmbZIP1* in soybean (*Glycine max*) (Gao *et al*., 2011), *ThbZIP1* in *Tamarixhispida* (Ji *et al*., 2013), *CaBZ1* in hot pepper (*Capsicum annuum*) (Moon *et al*., 2015), and *PtrABF* in trifoliate orange (*Citrus trifoliata*) (Zhang *et al*., 2015).

In order to improve the typically poor drought resistance of grapevines, researchers have focused their attention on the identification of drought-related TFs. Several, such as *CBF1/2/3/4* (Xiao *et al*., 2006; Siddiqua and Nassuth, 2011; Li *et al*., 2013), *WRKY11* (Liu *et al*., 2011a), *ERF1/2/3* (Zhu *et al*., 2013), *NAC26* (Fang *et al*., 2016), and *PAT1* (Yuan *et al*., 2016), have been identified and their overexpression in *A. thaliana* has been shown to enhance drought resistance. However, to date, only a few grapevine bZIP TFs have been functionally characterized during a drought stress response (Gao *et al*., 2014; Tu *et al*., 2016a, b), and their regulatory mechanisms are not well understood.

In this current study, we cloned a group A bZIP TF, *VlbZIP30*, from 'Kyoho' grapevine (*Vitis labrusca*×*V. vinifera*) and ectopically expressed it in *A. thaliana*. The results of physiological and transcriptomic analyses of the transgenic lines are presented and its putative function in drought-responsive signaling via the ABA signaling pathway in grapevine is discussed.

Materials and methods

Plant material and growth conditions

The two-year-old 'Kyoho' grapevine (*Vitis labrusca*×*V. vinifera*) plants used in this study were grown in the grapevine repository of the Northwest A&F University, Yangling, Shaanxi, China. *A. thaliana* ecotype Columbia (Col-0) plants used as both wild type (WT) and for transgenic experiments were grown in a greenhouse at 21°C under long-day (LD) conditions (16 h light/8 h dark).

Dehydration stress and ABA treatment of grapevine leaves

For dehydration treatments, grapevine shoots with three well-developed leaves were detached and immediately placed on dry filter paper in an illumination incubator at 25°C, with a relative humidity of 60-70%, under LD conditions (16 h light/8 h dark). For ABA treatments, leaves were sprayed with 100 μM ABA while the shoots were immersed in water, and the plants were then placed under the same ambient

conditions as above. Leaves from the same position were collected from three independent replicates of each treatment at 1, 2, 4, 6, 9, 12, and 24 h after initiating treatment. The 0 h samples were collected before each treatment was initiated and used as control samples. All samples were immediately frozen in liquid nitrogen and stored at −80°Cuntil further analysis.

Bioinformatic analysis

Full-length amino acid sequences of bZIP TFs from *A. thaliana* and grapevine were obtained from The Arabidopsis Information Resource (TAIR; http://www.arabidopsis.org/index.jsp) and EnsemblPlants (http://plants.ensembl.org/index.html), respectively. Multiple amino acid sequence alignments were generated using DNAMAN software (Version 5.2.2.0, LynnonBiosoft, USA) with default parameters, and a phylogenetic tree was constructed using the neighbor-joining (NJ) method and MEGA software (version 5.05), with 1,000 bootstrap replicates, as previously described (Tu *et al.*, 2016b). The predicted phosphorylation sites (C1, C2, C3, and C4) and highly conserved bZIP domain were analyzed as previously described (Fujita *et al*., 2005).

Transformation and characterization of transgenic plants

The plant transformation vectors 35S:*VlbZIP30* and Pro$_{VlbZIP30}$:*GUS* (β-glucosidase, details of vector construction are supplied in Supplementary Method S1) were transformed into *A. thaliana* by the floral dip method using *Agrobacterium tumefaciens* (strain GV3101) (Clough and Bent, 1998).

For each construct, seeds of the T0 and T1 plants were screened on Murashige-Skoog (MS) agar medium supplemented with 100 mg/L kanamycin. For phenotypic investigation, the three T3 homozygous lines (OE1, OE6 and OE23) with the highest levels of *VlbZIP30* expression, were used. To assess the expression of *GUS* in the Pro$_{VlbZIP30}$:*GUS* transgenic plants, T3 homozygous lines from 3 independent transgenic lines were analyzed. Seeds from each of the three selected T3 homozygous lines and from WT plants were vernalized and sterilized as previously

174 described (Tu *et al*., 2016b).

175

176 *Histochemical GUS assay*

177 An *in situ* GUS activity assay was performed as previously described (Tu *et al*.,
178 2016b).

179

180 *Osmotic stress and ABA treatment of transgenic seedlings*

181 WT and transgenic seeds were harvested at the same time. For seed germination and
182 cotyledon greening analyses, approximately 100 seeds from WT and each
183 35S:*VlbZIP30* line (OE1, OE6 and OE23) were grown on MS agar medium, MS agar
184 medium containing 300mM or 350 mM mannitol, or on MS agar medium containing
185 0.5 μM or 1 μM ABA, at 21°C with a 16 h light/8 h dark cycle. Germination and
186 cotyledon greening rates were defined as the obvious emergence of the seedling
187 radicle through the seed coat and green coloration of cotyledons, respectively (Tu *et*
188 *al*., 2016b). The seedlings were sampled after counting to measure the endogenous
189 ABA contents.

190 For the osmotic stress and ABA treatments, 7-day-old WT and transgenic
191 seedlings were transferred from MS medium plates into MS agar medium, or MS agar
192 medium supplemented with 300 mM or 350 mM mannitol, or MS agar medium
193 supplemented with 50 μM or 100 μM ABA. The root lengths were measured 7 d after
194 the transfer.

195

196 *Transcriptome analysis and identification of differentially expressed genes (DEGs)*

197 Seeds from WT and transgenic lines were cultivated on MS agar medium, with or
198 without stress treatment (0.5 μM ABA or 300 mM mannitol) for 7 d, and collected for
199 RNA extraction. For each RNA purification biological replicate, 300 seedlings of WT
200 or the OE lines from three MS agar plates were pooled to form a single sample. Three
201 independent RNA samples were used for each experiment.

202 Total RNA was extracted using the E.Z.N.A. Plant RNA Kit (Omega Bio-tek,
203 USA, R6827-01) according to the manufacturer's protocol (Invitrogen). RNA

concentration and integrity were confirmed using a NanoDrop 2000 spectrophotometer (Thermo Fisher Scientific, Wilmington, DE, USA) and an Agilent 2100 Bioanalyzer (Agilent Technologies, CA, USA). The construction of RNA-Seq libraries and sequencing were performed by the Biomarker Biotechnology Corporation (Beijing, China). The libraries were generated using the NEBNext UltraTM RNA Library Prep Kit for Illumina (NEB, USA) following the manufacturer's recommendations. Sequencing of the purified libraries was carried out using an Illumina HiseqXten platform (Illumina, NEB, USA) generating paired-end reads. The raw reads were cleaned by removing reads containing adapter sequences, reads containing poly-N and low quality reads. The cleaned reads from each sample were aligned to the *A. thaliana* reference genome from TAIR using the Tophat2 software (Kim *et al*., 2013). Gene expression levels were determined by fragments per kilobase of transcript per million fragments mapped (FPKM), and the DEGs were identified using edgeR software (Robinson *et al*., 2010), with a threshold of false discovery rate (FDR)<0.05 and absolute log2FC (fold change)>1. All raw sequence data in this study have been submitted to the NCBI Short Read Archive (SRA) under BioProject accession number PRJNA419694.

Transcriptome data analysis

The Venn diagrams were made using the BMK Cloud platform (www.biocloud.net). Annotations for DEGs were retrieved from TAIR. Gene Ontology (GO) enrichment analyses were performed for the functional categorization of DEGs based on the PageMan profiling tool (Usadel *et al.*, 2006) and Arabidopsis Functional Modules Supporting Data (Heyndrickx and Vandepoele, 2012). The grapevine orthologs of the *A. thaliana* genes were identified using TBLASTX software (Altschul *et al.*, 1997) with the highest score. Motif predictions were performed using the promoter region 1,500bp upstream of the start codons of the *A. thaliana* (AT) and grapevine (VIT) genes using DREME software (http://meme-suite.org/tools/dreme). The heat maps were constructed using HemI software (Deng *et al*., 2014). To identify the predicted grapevine genes, two grapevine-related ABA (Pilati *et al*., 2017) and drought stress

(Rocheta *et al*., 2016) databases were downloaded from the National Center for Biotechnology Information (NCBI) under BioProject accession number PRJNA369777 and the Gene Expression Omnibus (GEO) database under the number GSE57669.

Water loss assay and drought treatment of mature transgenic seedlings

For the water loss assay, rosette leaves of 3-week-old WT and transgenic plants were detached and immediately placed on dry filter paper. The samples, together with the paper, were then placed in the laboratory at ambient temperature with a relative humidity of 45-50%, and weighed at the indicated times. The fresh weight of the leaves was measured every 30 min to calculate relative water loss. The leaves were sampled after dehydration to examine cell death phenotypes, measure endogenous ABA content, antioxidant enzyme activity, and levels of ROS. The 0 h samples collected before dehydration were used as the negative control. For the drought treatment, plants were initially grown for 3 weeks under a normal watering regime and then water was withheld for 8 d. Survival rates were scored after re-watering for 3 days. Well-watered plants were used as the negative control.

Analysis of electrolyte leakage, MDA content, cell death, reactive oxygen species (ROS) levels, antioxidant enzyme activity and ABA content

The relative electrolyte leakage, MDA content and antioxidant enzyme activity were measured as previously described (Tu *et al*., 2016b), as was ABA content (Tu *et al.*, 2016a). Histochemical staining procedures were used to detect *in situ* reactive oxygen species (ROS) levels and dead cells as previously described (Tu *et al*., 2016b).

Stomatal aperture analysis

Stomatal aperture assays were performed as previously described (Tu *et al.*, 2016b).

RNA extraction and quantitative real-time PCR (qRT-PCR)

Total RNA was extracted from the grapevine leaves at 8 time points (0, 1, 2, 4, 6, 9,

12, and 24 h) after ABA and dehydration treatment using the E.Z.N.A._Plant RNA Kit (Omega Bio-tek, USA, R6827-01) following the manufacturer's instructions, as was total *A. thaliana* RNA from the leaves of 3-week-old WT and OE lines collected before and after dehydration. The qRT-PCR analyses were conducted using SYBR Premix Ex Taq II (TliRNaseH Plus) (TaKaRa Biotechnology) and a StepOnePlus™ RT-PCR instrument from Thermo Fisher Scientific with the following thermal profile: 95°C for 30 s, 45 cycles of 95°C for 5 s, and 60°C for 30 s. The expression levels of the grape *ACTIN1* (VIT_04s0044g00580) or *A. thaliana ACTIN2* (AT3G18780) genes were used as references. The specific primers for qRT-PCR are listed in Supplementary Table S1. Relative expression levels were analyzed using the StepOnePlus software (v. 2.3) and the Normalized Expression Method.

Statistical analysis

Data analysis was performed using Microsoft Excel (Microsoft Corporation, USA). The data were plotted using Sigmaplot (v. 10.0, Systat Inc., CA, USA). Paired t tests were performed to assess significant differences using the SPSS Statistics 17.0 software (IBM China Company Ltd., Beijing, China). All experiments were repeated three times as independent analyses.

Results

Identification of VlbZIP30, a group A bZIP TF from grapevine

The *VlbZIP30* (VIT_13s0175g00120) cDNA is 978 bp long and encodes a protein of 325 amino acids. Amino acid sequence analysis showed that, in common with the 8 members of the *A. thaliana* ABF/DPBF bZIP subfamily, VlbZIP30 also contains a leucine zipper domain (Jakoby *et al*., 2002) and conserved domains predicted as phosphorylation sites (C1, C2, C3 and C4) involved in drought stress or ABA signaling (Fujita *et al*., 2005) (Fig. 1). A phylogenetic analysis indicated that VlbZIP30 is most closely related to the group A ABF/DPBF TFs, which have previously been shown to be involved in ABA and drought stress signaling in *A.*

293 *thaliana* (Kang *et al*., 2002; Kim *et al*., 2002; Fujita *et al*., 2005; Yoshida *et al*., 2015),
294 and in grapevine (Nicolas *et al*., 2014; Tu *et al*., 2016a) (Fig. 2A).
295
296 *Expression of VlbZIP30 is induced by drought and ABA treatment*
297 To test whether *VlbZIP30* is involved in ABA and drought stress signaling, we first
298 evaluated the expression levels of *VlbZIP30* in grapevine following ABA or
299 dehydration treatments using qRT-PCR. As shown in Fig. 2B, ABA caused an increase
300 in *VlbZIP30* expression at 4 h and 6 h shortly after initiation of the treatment. The
301 expression peaked at 12 h, before decreasing for the next 24 h. Dehydration caused an
302 increase in *VlbZIP30* expression at 24 h.
303 Next, to investigate the temporal and spatial expression patterns of *VlbZIP30* in
304 more detail, histochemical GUS reporter experiments were performed with plants
305 grown under ABA and dehydration stress, as well as under normal conditions. Low
306 levels of GUS staining were observed in 2-d seeds at the germination stage , as well
307 as in 7 d and 14 d old seedlings (Fig. 2C, a, d and g), and GUS activity was
308 significantly enhanced after mannitol (Fig. 2C, b, e and h) and ABA (Fig. 2C, c, f and
309 i) treatments at the same stages. In mature plants, GUS staining was obviously
310 detected in stems, trichomes, flowers and siliques (Fig. 2C, n–q), while only slight
311 staining was detected in leaf petioles (Fig. 2C, j), and no staining was detected in
312 guard cells (Fig. 2C, l). However, after dehydration for 2 h, the leaf petioles and guard
313 cells showed an increase in GUS staining in 3-week-old plants (Fig. 2C, k, m). The
314 dehydration treatments had no effect on the size of the stomatal aperture. These
315 results suggest that *VlbZIP30* expression is regulated by ABA and drought stress.
316
317 *Overexpressing VlbZIP30 in A. thaliana reduces mannitol and ABA sensitivity during*
318 *seed germination and post-germination growth*
319 Three homozygous transformed lines (OE1, OE6 and OE23) with the highest levels of
320 *VlbZIP30* expression were selected based on qRT-PCR analysis (Supplementary Fig.
321 S1). Sterilized seeds of the transgenic lines and WT plants were cultivated on MS agar
322 medium, or MS agar medium containing 300 mM or 350 mM mannitol, or 0.5 μM or

1 μM ABA. The seed germination rates of the transgenic lines were not different to the rates observed for the WT when grown on MS agar medium for 3 d. However, the transgenic lines showed 20–32% and 6–13% higher seed germination than WT plants after mannitol (300 mM and 350 mM) and ABA (0.5 μM and 1 μM) treatments, respectively (Supplementary Fig. S2A, B). Given that ABA controls seed germination, and that its biosynthesis can be affected by abiotic stress (Iuchi *et al*., 2001; Fujii and Zhu, 2009), we measured endogenous ABA contents. We found that ABA levels in the transgenic lines were slightly higher than in WT following mannitol or ABA treatments (Supplementary Fig. S2C).

We also examined cotyledon greening rates in plants grown on MS agar medium for 7 d and observed that the transgenic lines and WT showed no significant differences (Fig. 3A). However, the transgenic lines showed 30–39% and 19–20% higher cotyledon greening rates than WT plants after 7 d with mannitol (300 mM and 350 mM) and ABA (0.5 μM) treatments, respectively (Fig. 3B). The cotyledon greening rates of both transgenic lines and WT decreased substantially in response to the 1 μM ABA treatment, but the transgenic seedlings exhibited 4–6% higher cotyledon greening rates than the WT (Fig. 3A, B). The cotyledon greening rates were further tested at different time points after treatment with 350 mM mannitol or 1 μM ABA. As shown in Fig. 3C, neither the transgenic lines nor WT plants had greening cotyledons 3 d after treatment with 350 mM mannitol. However, the cotyledon greening rates of the transgenic lines were significantly higher than those of WT 4 d after treatment, and gap gradually increased with time, and peaked at 7 d. When grown on MS agar medium supplied with 1 μM ABA, the cotyledon greening rates of transgenic lines and WT showed no significant difference at 6, 7 and 8 d, while the transgenic lines exhibited 11–12% and 29–35% higher cotyledon greening rates than WT plants 9 d and 11 d after treatment, respectively (Fig. 3D). These results suggest that over-expressing *VlbZIP30* reduced sensitivity of *A. thaliana* seedlings to mannitol and ABA. In addition, the endogenous ABA levels in the transgenic lines were higher than those in WT after exposure to 350 mM mannitol (Fig. 3E), suggesting that the transgenic plants were insensitive to mannitol, possibly due to

353 altered endogenous ABA levels.

354 To further characterize morphological changes of WT and transgenic seedlings in
355 response to the mannitol and ABA treatments, the various seed genotypes described
356 above were grown on MS agar medium, with or without 300 mM mannitol, or 0.5 μM
357 ABA for 14 d. As shown in Fig. 4A, the size of cotyledons and roots of the transgenic
358 seedlings were significantly bigger and longer than those of WT following both
359 treatments, while there was no differences observed under control conditions.

360 To determine whether the transgenic lines had longer primary roots as a
361 consequence of precocious germination or development of post-germination growth,
362 7-d-old transgenic lines and WT seedlings grown on MS agar medium were
363 transferred to MS agar medium with or without mannitol or ABA, and grown for
364 another 7 d. When grown on MS agar medium, the primary root lengths were similar;
365 however, when grown on MS agar medium containing mannitol (300 mM and 350
366 mM) or ABA (50 μM and 100 μM), the transgenic lines had relatively longer primary
367 roots than WT seedlings under mannitol treatment, while there was no significant
368 difference in response to the ABA treatment (Fig. 4B, C). This indicated that
369 *VlbZIP30* plays a role in suppressing the retardation of germination mediated by ABA,
370 but not in root growth inhibition.

371 One effect of osmotic stress is membrane lipid peroxidation, and the levels of
372 electrolyte leakage and malondialdehyde (MDA) are often used as indicators of the
373 degree of cell membrane injury and tissue damage (Neill *et al.*, 2002; Pompelli *et al.*,
374 2010). We measured electrolyte leakage and MDA levels in the transgenic and WT
375 seedlings after 300 mM or 350 mM mannitol treatment and saw that under normal
376 growth conditions, there was no significant difference between the transgenic lines
377 and WT seedlings. However, following treatments with different mannitol
378 concentrations, the values in the transgenic lines were significantly lower than in WT,
379 indicating that the degree of membrane and tissue damage was less as a result of
380 *VlbZIP30*-overexpression (Fig. 4D, E). Taken together, these results indicated that
381 overexpressing *VlbZIP30* in *A. thaliana* enhanced osmotic stress tolerance not only at
382 the germination stage, but also during post-germination developmental processes.

The expression of many ABA- or drought-responsive genes is induced in VlbZIP30-overexpressing lines

To examine the possible roles of *VlbZIP30* in transcriptional regulation in response to ABA and osmotic stress, we performed a global transcriptome analysis to identify DEGs between the WT and *VlbZIP30*-overexpressing lines using RNA-seq. Seeds from WT and OE1 transgenic lines were cultivated on MS agar medium with or without 0.5 μM ABA or 300 mM mannitol for 7 d, and the seedlings were then collected for transcriptome analysis (Fig. 3A, scheme summarized in Fig. 5A). DEGs were defined based on a threshold of 2-fold change (FDR<0.05). We identified 10 genes that were up- and 10 that were down-regulated in the OE lines compared with WT plants under control conditions (OEC / WTC, Fig. 5B, C). Details of these 20 genes, including their annotation and their expression levels are listed in Supplementary Table S2. After treatments, a total of 1,735 and 2,203 up-regulated genes and 1,734 and 1,764 down-regulated genes were identified in WT plants subjected to ABA (WTA / WTC) and mannitol (WTM / WTC) stress, respectively (Fig. 5B, C). A total of 1,510 and 1,494 up-regulated genes, and 1,058 and 729 down-regulated genes were found in the OE lines subjected to ABA (OEA / OEC) and mannitol (OEM / OEC) stress, respectively (Fig. 5B, C). We also identified 359 and 139 genes that were up- and down-regulated, respectively, in the OE lines compared with WT plants when treated with ABA (OEA / WTA, Fig. 5B, C), while 783 and 344 genes were up- and down-regulated, respectively, when treated with mannitol (OEM / WTM, Fig. 5B, C).

To deduce the possible functions of the *VlbZIP30*-induced genes, we performed a gene ontology (GO) analysis of the genes, whose expression levels were significantly altered in the OE lines compared with the WT plants in response to ABA (OEA / WTA) or mannitol stress (OEM / WTM), using the PageMan profiling tool (Usadel *et al*., 2006). This revealed that some genes encode TFs, and some genes are putatively involved in photosynthesis, stress, signaling, transport, development and several other metabolic pathways involving hormones, amino acids and lipids (Fig. 6).

To better understand the role of *VlbZIP30* in ABA and osmotic stress signaling, the OEA / OEC and OEA / WTA intersecting genes (up-regulated genes, 29+53; down-regulated genes, 8+11) and the OEM / OEC and OEM / WTM intersecting genes (up-regulated genes, 47+115; down-regulated genes, 5+16) were selected for further analysis (Fig. 5B, C). We identified all of the 248 (210 up-regulated genes, 38 down-regulated genes) genes mentioned above, and found that 38% (95/248) genes had been identified in *A. thaliana*. Among them, 54 genes were involved in abiotic stress, including stress-responsive genes (*RD20*, *RD22*, *RD26*, *SIS* and *ERD10*), ABA signaling genes (*AFP1*, *AFP3*, *HB7*, *HB12*, *NCED3*, *MAPKKK18*, *PYL6*), PP2C genes (*ABI1*, *ABI2*, *HAI1*, *HAI2*, *HAB1* and *PP2CA*), TFs (*ABF2*, *ABF3*, *ABF4*, *DREB1A*, *NFYA5*, *NFYB2*, *NAP*, *MYB74*, *WRKY28*, *ERF053* and *bHLH129*), and others (Table 1). The other 41 genes were involved in other processes such as wax biosynthesis (*ABCG19*), photosynthesis, transport, hormone signaling (brassinosteroids, ethylene and cytokinins), mineral homeostasis (Fe, Ca, Pi and S) and others (Supplementary Table S3). We noted that the genes involved in hormone signaling were almost all down-regulated in the OE lines compared with WT plants in response to both treatments, while the genes involved in mineral homeostasis were almost all up-regulated in the OE lines compared with WT plants following ABA treatment (Supplementary Table S3). To date, the functions of these genes characterized in Arabidopsis were consistent with the results of GO analysis (Fig. 6).

To confirm the RNA-seq results, we examined the expression of 20 drought-responsive genes by qRT-PCR and saw that the expression changes of all these genes were similar in the RNA-seq and qRT-PCR data. As shown in Fig. 7, the expression of four stress-marker genes and six ABA signaling genes, but not *NCED3*, was up-regulated during both treatments in OE lines compared with WT plants. There were increased transcript levels of the ABA biosynthesis related gene *NCED3* in the OE lines during mannitol stress, which correlated with the endogenous ABA content (Fig. 3E). Furthermore, the expression of several marker genes in the core ABA signaling network, including PP2Cs and *PYL6*, also showed significant change. Specifically, the expression of 4 PP2Cs significantly increased in the OE lines relative

443 to WT plants, while the expression of *PYL6* decreased in OE lines compared with WT
444 plants during mannitol stress.
445
446 *The presence of a potential G-box motif in VlbZIP30 induced genes*
447 To identify candidate *VlbZIP30* target genes, promoter analyses of the DEGs between
448 OE lines and WT plants under control conditions (10 up-regulated and 10
449 down-regulated genes) and during ABA or mannitol treatment (210 up-regulated and
450 38 down-regulated genes) were performed using the DREME motif discovery tool.
451 All up-regulated and all down-regulated genes were divided in two clusters performed
452 promoter analyses, respectively. Excitingly, We identified a potential G-box
453 *cis*-element motif (ACGTGKV; E-value, 2.5e-017) including a 4-bp core sequence
454 (ACGT) that is known to be a bZIP binding motif, as being significantly enriched in
455 the promoters of the up-regulated genes (Fig. 8A), in that 85% (187/220) carried this
456 motif in their upstream 1,500 bp promoter region. The G-box motif was not enriched
457 in the down-regulated genes. We next analyzed the number and location of the G-box
458 motifs in the 187 gene promoters, and observed that many genes carried 1 to 3 G-box
459 motifs, and that the highest G-box frequency was within the first 300 bp from the start
460 codon site (Fig. 8C, E).
461 ABRE (PyACGTGGC) and G-box (CACGTG) elements have previously been
462 identified as *cis*-binding elements for bZIP proteins that regulate gene expression in
463 response to ABA or drought stress in many plants, such as *A. thaliana* (Uno *et al*.,
464 2000), rice (Liu *et al*., 2014), wheat (Wang *et al*., 2016), soybean (Liao *et al*., 2008),
465 tomato (Hsieh *et al*., 2010), maize (Zhang *et al*., 2011), orange (Zhang *et al*., 2015),
466 potato (Muniz Garcia et al., 2012), and *Tamarixhispida* (Ji *et al*., 2015). We searched
467 the grapevine genome for homologs of the identified *A. thaliana* up-regulated (220)
468 and down-regulated (48) genes (Fig. 5D, E; Supplementary Data S1) and a promoter
469 analysis performed using the DREME motif discovery tool. Homologs were found of
470 195 of the up-regulated and 44 of the down-regulated genes (Supplementary Data S1).
471 Using the same analytical method, surprising, a potential G/C-box *cis*-element motif
472 (MCACGTS; E-value, 8.3e-018) including the core sequence (ACGT) was found to

be significantly enriched in the homologs to the up-regulated genes (Fig. 8B). We determined that 55% (108/195) of the up-regulated genes had at least one G/C-box motif in their upstream 1,500 bp promoter region, while this motif was not enriched in the down-regulated genes. Many of the 195 genes carried 1 or 2 G/C box motifs, and the highest frequency was seen in these quence up to 300 bp from start codon site (Fig. 8D, F), similar to the *A. thaliana* genes (Fig. 8C, E).

Next, those genes with three or more G-box (*A. thaliana*) or G/C-box (grapevine) motifs were selected (Piya *et al*., 2017). We found that 52% (97/187) of the *A. thaliana* genes and 50% (54/108) of the grapevine genes had at least three motifs and that all of the latter had G-box, but not C-box motifs. We scanned the above-mentioned 97 *A. thaliana* genes and 54 grapevine genes containing three or more G-box motifs, and found that 61 of the *A. thaliana* genes were homologous to one of the 54 grapevine genes. Of the 97 and 61 *A. thaliana* genes, we identified 39 with three or more G-box motifs in their promoters by Venn diagram (Fig. 9A). Another DREME promoter analysis of these 39 genes revealed 4 enriched motifs, including a perfect G-box (CACGTG, E-value: 9.0e-012), a GAGA-box (DAGAGAGA, E-value: 1.1e-005), an AAGAAAAR motif (E-value: 7.9e-004), and a TATA-box (ABATATAT, E-value: 9.9e-004) (Fig. 9B). The frequencies of the G-box in the *VlbZIP30*-induced 39 and 220 *A. thaliana* genes were 89.7% and 70.0%, respectively, while the frequency in the whole genome was 51.5%, suggesting an enrichment in the *VlbZIP30* induced genes. Such an enrichment was not found for the other three motifs (Fig. 9B).

In grapevine, 88 homologs of the 97 *A. thaliana* genes were found. Among the 88 and 54 grapevine genes, we identified 35 with at least three G-box motifs in their promoters by Venn diagram (Fig. 9C). Three enriched motifs, including a potential grapevine G-box (MCACGTGK, E-value: 1.9e-009), a GAGA-box (RAGAGARA, E-value: 2.4e-007), and a CACSTC (E-value: 3.5e-004) motif were identified in these 35 genes (Fig. 9D). Among them, the frequencies of the G-box in the predicted *VlbZIP30*-induced 35 and 196 grapevine genes were 100.0% and 77.4%, respectively, while the frequency of the G-box in the whole genome was 59.0%, again indicating

503 an enrichment in the predicted *VlbZIP30* induced genes. These results suggest that the
504 35 grapevine genes may be regulated by *VlbZIP30* via the potential G-box. The names
505 and gene IDs of the 35 grapevine genes and 39 *A. thaliana* genes are listed in
506 Supplementary Data S2.
507
508 *The expression of the predicted VlbZIP30 induced genes with at least three potential*
509 *G-box motifs was up-regulated in grapevine following both ABA and drought*
510 *treatments*
511 To investigate the potential roles of the 35 identified grapevine genes in ABA and
512 drought stress, two different grapevine-related databases for ABA (Pilati *et al.*, 2017)
513 and drought (Rocheta *et al.*, 2016) stress treatments were analyzed. RNA-seq analysis
514 was performed of grapevine berry skins with or without ABA treatment for 20 h and
515 44 h. A GrapeGene GeneChips® data analysis was performed of leaves from two *Vitis*
516 *vinifera* L. varieties (Trincadeira, TR and Touriga Nacional, TN) grown under control
517 and drought greenhouse conditions, as well as fully irrigated and non-irrigated field
518 conditions. We compared the genes in those datasets with the 35 predicted grapevine
519 genes, and found that 31 and 25 appeared in the RNA-seq and GeneChips® data (Fig.
520 10A). Of these, 74% (23/31) and 84% (21/25) were significantly up-regulated
521 following the ABA and drought treatments, respectively (Fig. 10A). Six genes only
522 responded to ABA and 4 only responded to drought, and 17 responded to both
523 treatments (Fig. 10A). The detailed expression data for these 27 genes (Fig. 10A) are
524 shown in heat map diagrams in Fig. 10B.
525 We randomly selected 16 genes of the 27 genes induced by ABA or drought
526 stress, for confirmatory qRT-PCR expression analysis, using the previously mentioned
527 grapevine leaf samples subjected to ABA or dehydration treatment. The results were
528 consistent with the results previously published (Fig. 10C; Supplementary Fig. S3).
529 Interestingly, *ABF2/bZIP39* (VIT_18s0001g10450), which was characterized as being
530 involved in ABA signaling in grapevine cell culture, has been reported to transiently
531 trans-activate the expression of *NAC17* (VIT_19s0014g03290) and *PUB19*
532 (VIT_17s0000g08080) following ABA treatment (Nicolas *et al.*, 2014; Pilati *et al.*,

2017). In addition, overexpression of this gene in *A. thaliana* enhances tolerance to drought stress through the ABA signaling pathway (Tu *et al*., 2016a), suggesting that *NAC17* and *PUB19* may enhance drought stress in grapevine.

VlbZIP30 overexpressing A. thaliana lines showed enhanced dehydration tolerance at the adult stage

To further investigate the potential function of *VlbZIP30* in dehydration stress, the *VlbZIP30*-overexpressing (OE1, OE6 and OE23) lines and WT plants were grown for 3 weeks under normal growth conditions and then exposed to dehydration stress by withholding water for 8 d. All of the WT plants showed severe wilting symptoms, while only slight wilting was observed in the OE lines (Fig. 11A). Only 25% of the WT plants recovered after 3 d of rehydration, while the OE lines rapidly recovered, and 69–94% of the OE lines survived (Fig. 11A). We excised the aerial parts of the OE lines and WT plants and water loss was examined over time. The OE lines lost water more slowly than WT plants (Fig. 11B, C) and, consistent with the visible phenotypes, when leaves were stained with trypan blue, those of WT showed a deeper staining than those of the OE lines (Fig. 11B), suggesting a higher rate of cell death after 3 h dehydration. Since ROS triggered by drought stress can cause oxidative damage to cellular membranes, and ultimately result in cell death (You *et al*., 2014), we measured ROS levels, as well as the activities of antioxidant enzymes (SOD, CAT and POD) in WT and OE lines before and after dehydration for 3 h. WT plants accumulated more ROS and had lower antioxidant enzyme activities than OE lines after 3 h dehydration (Supplementary Fig. S4), consistent with the cell death data. These results suggest that *VlbZIP30* promotes dehydration stress responses.

It has been reported that some guard cells of drought-tolerant plants are hypersensitive to ABA (Fujita *et al*., 2005; Sakuraba *et al*., 2015), and this prompted us to test whether the enhanced dehydration resistance of the OE lines was associated with ABA-regulated stomatal closure. We measured stomatal aperture in the leaves of 3-week-old WT and OE lines in the presence of 10 μM ABA, but after 1 h of ABA treatment, no significant difference was observed (Supplementary Fig. S5). We then

563 measured the endogenous ABA content before and after dehydration and while there
564 was no difference under normal conditions, the ABA content of the OE lines was
565 higher than in WT plants after dehydration for 1 h or 2 h (Fig. 11D). These results
566 suggested that the OE lines had enhanced drought resistance due to ABA signaling,
567 but not because of ABA-regulated stomatal closure.

568 Subsequently, by reading a large number of articles and analyzing the
569 transcriptome data, we identified 6 genes (*MYB94*, *MYB96*, *KCS6*, *KCS12*, *LACS3*,
570 and *ABCG19*) involved in cuticular wax biosynthesis that were significantly
571 up-regulated in the OE lines compared with WT plants under mannitol stress (Table 1;
572 Supplementary Table S3). Previous studies showed that *A. thaliana* can adapt to
573 drought stress through *MYB94*- and *MYB96*-mediated regulation of cuticular wax
574 biosynthesis via a downstream branch of the ABA core signaling pathway that is
575 different from the stomata closure sub-branch of ABA signaling (Seo *et al*., 2011; Cui
576 *et al*., 2016; Lee *et al*., 2016a). Seo *et al*. (2011) suggested that the *MYB96* TF
577 promotes drought resistance by regulating cuticular wax biosynthetic genes (including
578 *KCS6*, *KCS12*, *LACS3*, and *ABCG19*) in the ABA-dependent pathway. We found that
579 the expression of *MYB96* gradually increased after 1 and 2 h of dehydration stress in
580 both WT and OE lines, but that it significantly increased in the OE lines compared
581 with the WT (Fig. 11E). The expression level of *KCS6*, a *MYB96* direct binding target
582 (Seo *et al*., 2011; Lee *et al*., 2016a), showed the same trend. The expression of
583 another cuticular wax biosynthetic gene, *LACS3*, was also up-regulated in the OE
584 lines compared with WT after dehydration for 1 h. However, the expression levels of
585 the stress-marker genes, *RD20*, *RD26* and *ERD10*, were not significantly different
586 between WT and OE lines in response to dehydration. *AFP1* and *AFP3*, which encode
587 ABI five binding proteins, regulate the drought response in germinating *A. thaliana*
588 seeds and seedlings, and their mutation results in ABA hypersensitivity (Garcia *et al*.,
589 2008). We observed that the expression of these genes significantly increased in OE
590 lines compared with WT after 2 h of dehydration stress. The expression of the ABA
591 core signaling network genes *ABI1*, *HAI1*, *HAI2* (PP2Cs), and *PYL6* was also
592 measured, and while *HAI1* and *HAI2* were significantly up-regulated in the OE lines

after 2 h of dehydration stress, the expression of *PYL6* was significantly down-regulated. *HB7* and *HB12*, which are positive transcriptional regulators of PP2Cs, suppress the transcription of *PYL5* and *PYL8* in response to ABA, and enhance drought tolerance as mediators of a negative feedback effect on ABA signaling in *A. thaliana* (Valdes *et al*., 2012). Here, we found that the expression of *HB7* was up-regulated in the OE lines after 1 h of dehydration stress compared with the WT. In addition, transcript levels of the ABA biosynthesis marker gene, *NCED3*, were higher in the OE lines after 1 h or 2 h of dehydration stress compared with the WT. Finally, the expression of *ABF3*, a key TF involved in the ABA signaling pathway (Kang *et al.*, 2002), significantly increased in the OE lines after 2 h of dehydration stress compared with the WT.

Finally, to investigate whether cuticular wax biosynthetic genes were induced by dehydration stress in grapevine, we examined the transcript levels of *KCS6* (VIT_14s0006g02990) and *LACS4* (VIT_02s0025g01410), which are homologous to *A. thaliana KCS6* (AT1G68530) and *LACS3* (AT1G64400), and found both to be induced by dehydration stress, peaking at 24 h (Supplementary Fig. S3).

Discussion

Early studies identified three bZIP-type ABRE-binding proteins, *AREB1*, *AREB2* and *AREB3* from *A. thaliana*, using an ABRE motif (Uno *et al*., 2000), and *ABF3* and *ABF4/AREB2* were shown to play important roles in response to ABA and drought stress signaling (Kim *et al*., 2004) . *AREB1* enhances drought resistance in *A. thaliana*, involving the ABA signaling pathway (Fujita *et al*., 2005). In addition, Furihata *et al*. (2006) showed that exogenous ABA activates the SnRK2 protein kinases, and that the activated SnRK2 proteins phosphorylate a Ser/Thr residue in the conserved domains (C1, C2, C3 and C4) of the downstream *AREB1* gene, allowing it to bind to the *cis*-acting ABRE element of downstream drought-related genes. The mechanism involving *AREB1* in the ABA core signaling pathway in *A. thaliana* is also present in economically important crops, such as rice. For example, ABA and drought stress can

trigger a rice SnRK2 protein kinase to phosphorylate rice bZIP TF, *TRAB1*, a homolog of *A. thaliana AREB1* and *AREB2* (Kagaya *et al*., 2002; Kobayashi *et al*., 2005). Chae *et al*. (2007) found that another rice bZIP TF, *OREB1*, can also be phosphorylated by a SnRK2 family protein kinase, *OSRK1*. These studies suggest that similar regulatory responses to stress are evolutionarily conserved in plants.

In this study, we identified a group A bZIP TF, *VlbZIP30*, from grapevine. Phylogenetic analyses indicated that VlbZIP30 is most closely related to ABF/DPBF TFs of group A, with conserved domains predicted to contain phosphorylation sites (C1, C2, C3 and C4) (Fujita *et al*., 2005), suggesting that the *VlbZIP30* may be involved in drought stress and ABA core signaling (Fig. 1; Fig. 2A). Further work is still required to verify whether the conserved domains (C1, C2, C3 and C4) of VlbZIP30 are phosphorylated and that the protein is involved in the ABA core signaling pathway.

Previous studies have demonstrated that overexpressing drought-induced genes in *A. thaliana* can cause hypersensitivity to ABA and increase tolerance to drought stress (Fujita *et al*., 2005). In this study, overexpressing *VlbZIP30* in *A. thaliana* did not make the plants more sensitive to ABA, but increased their osmotic stress tolerance during germination and post-germination growth. Similar results were reported for *SAD1*, *AtTPS1*, *AtHD2C*, *CaXTH3*, *OsMYB3R-2* and *ABO3* (Xiong *et al*., 2001; Avonce *et al*., 2004; Cho *et al*., 2006; Sridha and Wu, 2006; Dai *et al*., 2007; Ren *et al*., 2010). Given that *VlbZIP30* is a TF, its role in osmotic stress response is likely to involve regulating downstream gene expression. Indeed, a majority of the ABA- and drought-induced genes tested were induced in *VlbZIP30*-overexpressing *A. thaliana* following ABA and mannitol treatment. Ninety-five (38%) of the 248 genes identified (Fig. 5) have previously been identified and of these 54 were involved in abiotic stress, including stress marker genes (*RD20*, *RD22*, *RD26* and others), ABA core signaling components (6 PP2Cs: *ABI1*, *ABI2*, *HAI1*, *HAI2*, *HAB1*, *PP2CA*, and *PYL6*), TFs (*ABF2*, *ABF3*, *ABF4* and others) (Table 1). Nine *A. thaliana* PP2Cs belonging to cluster A have been identified (Schweighofer *et al*., 2004), and studies have shown that 6 of them (*ABI1*, *ABI2*, *HAI1*, *HAI2*, *HAB1*, and *PP2CA*) function as

652 negative regulators of ABA signaling, with their mutants showing hypersensitivity to
653 ABA during seed germination and seedling growth (Merlot *et al*., 2001; Saez *et al*.,
654 2006; Yoshida *et al.*, 2006; Bhaskara *et al.*, 2012). In addition, the *ABI1*, *ABI2*, *HAI1*
655 and *HAI2* genes are known to act in a negative feedback regulatory loop of the ABA
656 signaling pathway (Merlot *et al*., 2001; Bhaskara *et al*., 2012). A sextuple mutant
657 impaired in six PYR/PYL receptors was shown to be very insensitive to ABA during
658 seed germination and seedling growth (Gonzalez-Guzman *et al*., 2012). Here, we
659 found that the transcript levels of the 6 PP2Cs were all significantly higher in the
660 *VlbZIP30*-overexpressing lines in response to osmotic stress, while the expression of
661 *PYL6* was lower (Table 1). Consistent with this, the OE lines were found to be
662 insensitive to ABA. These results suggested that *VlbZIP30* may play a role in the
663 ABA core signaling pathway under osmotic stress conditions, and be involved in a
664 negative feedback regulatory loop of the ABA signaling pathway in *A. thaliana* during
665 the seedling stage.

666 Previous studies have shown that guard-cell movement mediated by ABA is a
667 primary mechanism to prevent water loss under dehydration stress conditions (Kang
668 *et al*., 2002; Fujita *et al.*, 2005). In this study, we found the stomatal closure regulated
669 by ABA to be impaired in the OE lines (Supplementary Fig. S5), but that the
670 expression the stress-marker genes (*RD20*, *RD26* and *ERD10*) was not be
671 significantly different between the WT and OE lines. However, the expression levels
672 of cuticular wax biosynthesis genes (*MYB96*, *KCS6* and *LACS3*) were significantly
673 up-regulated in the OE lines compared with WT plants at the adult stage under
674 dehydration stress (Fig. 11E). In addition, the expression of *HB7* and two PP2C genes
675 (*HAI1* and *HAI2*), which are mediators of a negative feedback regulatory loop of the
676 ABA core signaling pathway in *A. thaliana* (Bhaskara *et al*., 2012; Valdes *et al*.,
677 2012), were up-regulated in the OE lines compared with WT plants under dehydration
678 stress (Fig. 11E). Our data suggest that overexpression of *VlbZIP30* enhances the
679 tolerance of *A. thaliana* to dehydration stress at the adult stage through regulating
680 cuticular wax biosynthesis related genes in the ABA signaling pathway. This is
681 consistent with previous studies (Seo *et al*., 2011; Cui *et al*., 2016; Lee *et al*., 2016a).

682 The ABRE (PyACGTGGC) and G-box (CACGTG) elements were identified as
683 bZIP TF *cis*-binding elements regulating gene expression in response to ABA and
684 drought stress in many plants, including *A. thaliana* (Uno *et al.*, 2000), rice (Liu *et al.*,
685 2014) and wheat (Wang *et al.*, 2016). In this study, we identified 39 *A. thaliana* genes
686 and 35 predicted grapevine genes (Supplementary Data S2) that may be directly or
687 indirectly regulated by *VlbZIP30*. Seventeen (43.6%) of the 39 *A. thaliana* genes have
688 been found to be involved in drought stress, including *RD26*, *AFP1/3*, *PP2CA*,
689 *HAI1/2*, *ABF3*, *NAP*, *MYB74*, *WRKY28* and *PUB19* (Table 1), implying that our
690 analytical methods and results are very credible. Other genes found here that have not
691 been previously characterized may therefore also be involved in drought stress
692 signaling. In contrast, there has been little characterization of the 35 grapevine genes,
693 and only 3 were identified as being involved in ABA or drought stress signaling.
694 *ABF2/bZIP39* (VIT_18s0001g10450), which has been associated with both stimuli
695 (Nicolas *et al.*, 2014; Tu *et al.*, 2016a), can transiently transactivate the expression of
696 *NAC17* (VIT_19s0014g03290) and *PUB19* (VIT_17s0000g08080) in response to
697 ABA treatment (Nicolas *et al.*, 2014; Pilati *et al.*, 2017).

698 A perfect *A. thaliana* G-box (CACGTG) and a putative grapevine G-box
699 (MCACGTGK) element were significantly enriched in the promoter of the 39 *A.*
700 *thaliana* genes and 35 predicted grapevine genes (Fig. 9B, D). The highly conserved
701 G-box motif (CACGTG) is regulated by bZIP TFs in organisms ranging from yeast to
702 humans (Ezer *et al.*, 2017). Ezer *et al.* (2017) constructed an available gene
703 expression network (www.araboxcis.org) for prediction of genes regulating the G-box,
704 or a set of genes regulated by the G-box. They identified approximately 2,000
705 seedling-expressed genes expressed in 229 RNA-seq samples of 7-d-old *A. thaliana*
706 seedlings that are highly likely to be regulated by a perfect G-box motif (CACGTG)
707 in their promoter, and predicted how bZIP proteins might regulate these genes.
708 These results suggest that *VlbZIP30* is likely to enhance *A. thaliana* drought tolerance
709 by regulating downstream genes containing a perfect G-box (CACGTG). Large-scale
710 transcriptome analyses also show that the G-box (CACGTG) was highly enriched in
711 stress-responsive genes in grapevines (Wong et *al.*, 2017). These results suggest a

general conservation in promoter framework, gene expression dynamics and gene regulatory networks. We also used two different grapevine-related databases to gain support for the potential roles of the 35 grapevine genes in ABA and drought stress.

We noted that 74% and 84% (a total of 27) candidate genes were significantly up-regulated under ABA or drought treatment, respectively (Fig. 10A, B), and that the expression of some of these genes was up to 64-fold induced (Fig. 10B). In addition, we found by qRT-PCR analysis that the expression levels of 16 randomly selected genes from the 27 genes (including *VvPP2C9*, *VvPP2C37* and *VvABF2*) were significantly up-regulated by ABA or dehydration treatment (Fig. 10C; Supplementary Fig. S3), suggesting that the 27 candidate genes may involve in ABA or dehydration stress in grapevine. These results suggest that *VlbZIP30* may be involved in drought stress signaling in grapevine via regulation of the 27 grapevine genes containing the grapevine G-box (MCACGTGK). This conclusion is supported by the observation that 17 of the 39 *A. thaliana* homologous genes have previously been found to be involved in drought stress. Further studies be required to elucidate the functions of these regulated ABA and drought stress regulated grapevine genes.

Supplementary data

Fig. S1. *VlbZIP30* mRNA levels in wild-type (WT) and transgenic plants analyzed by qRT-PCR.

Fig. S2. Phenotypes of wild type (WT) and *VlbZIP30* overexpressing transgenic lines at the seed germination stage under mannitol and abscisic acid (ABA) treatments.

Fig. S3. Gene expression profiles of selected *VlbZIP30*-induced grapevine candidate genes analyzed using qRT-PCR.

Fig. S4. Reactive oxygen species (ROS) levels and oxidative enzyme activities in wild type (WT) and transgenic lines (OE).

Fig. S5. Stomatal closure in response to 10 μM exogenous ABA in 3-week-old wild type (WT) and transgenic lines (OE).

Table S1. Specific primers used for qRT-PCR. F, forward; R, reverse.

741 Table S2. Differentially expressed genes in the *VlbZIP30* transgenic plants (OE / WT)
742 based on an expression level differences (FDR<0.05) of at least two-fold under
743 control conditions from the transcriptome data.
744 Table S3. Selected genes involved in other biological processes based on expression
745 level differences (FDR<0.05) of at least two-fold in the *VlbZIP30* transgenic plants
746 under ABA or mannitol stress treatment from the transcriptome data.
747 Data S1. Grapevine homologs of the up-regulated genes identified in *Arabidopsis*
748 *thaliana* OE lines compared with WT plants.
749 Data S2. Names and annotations of 35 grapevine genes and 39 *Arabidopsis thaliana*
750 genes.
751 Methods S1. Vector construction.
752

753 Author contribution

754 X. Wang and M. Tu designed the study. M. Tu and X.H. Wang contributed to the
755 experiments, X.H. Wang and D. Wang constructed the vectors, Y. Zhu performed the
756 qRT-PCR analysis, M. Tu and D. Wang performed data analysis. M. Tu, X.H. Wang,
757 X. Zhang and Y. Cui performed transcriptome data analysis, Z. Li, Y. Li and M. Gao
758 assisted with the data analysis. M. Tu and X. Wang wrote the manuscript. All of the
759 authors approved the final manuscript.
760

761 Acknowledgments

762 This work was supported by the National Natural Science Foundation of China
763 (31572110), as well as the Program for Innovative Research Team of Grape
764 Germplasm Resources and Breeding (2013KCT-25). We thank PlantScribe (www.
765 plantscribe.com) for careful editing of this manuscript.
766

References

Altschul SF, Madden TL, Schaffer AA, *et al*. 1997. Gapped BLAST and PSI-BLAST: a new generation of protein database search programs. Nucleic acids research **25**, 3389-3402.

Aubert Y, Vile D, Pervent M, *et al*. 2010. RD20, a stress-inducible caleosin, participates in stomatal control, transpiration and drought tolerance in Arabidopsis thaliana. Plant Cell Physiology **51**, 1975-1987.

Avonce N, Leyman B, Mascorro-Gallardo JO, *et al*. 2004. The Arabidopsis trehalose-6-P synthase AtTPS1 gene is a regulator of glucose, abscisic acid, and stress signaling. Plant Physiology **136**, 3649-3659.

Babitha KC, Ramu SV, Pruthvi V, *et al*. 2013. Co-expression of AtbHLH17 and AtWRKY28 confers resistance to abiotic stress in Arabidopsis. Transgenic research **22**, 327-341.

Bhaskara GB, Nguyen TT, Verslues PE. 2012. Unique drought resistance functions of the highly ABA-induced clade A protein phosphatase 2Cs. Plant Physiology **160**, 379-395.

Brauer EK, Ahsan N, Dale R, *et al*. 2016. The Raf-like Kinase ILK1 and the High Affinity K^+ Transporter HAK5 Are Required for Innate Immunity and Abiotic Stress Response. Plant Physiology **171**, 1470-1484.

Brinker M, Brosche M, Vinocur B, *et al*. 2010. Linking the salt transcriptome with physiological responses of a salt-resistant Populus species as a strategy to identify genes important for stress acclimation. Plant Physiology **154**, 1697-1709.

Buxdorf K, Yaffe H, Barda O, Levy M. 2013. The effects of glucosinolates and their breakdown products on necrotrophic fungi. PLoS One **8**, e70771.

Chae M-J, Lee J-S, Nam M-H, *et al*. 2007. A rice dehydration-inducible SNF1-related protein kinase2 phosphorylates an abscisic acid responsive elementbinding factor and associates with ABA signaling. Plant Molecular Biology, 63, 151-169.

Cho SK, Kim JE, Park JA, Eom TJ, Kim WT. 2006. Constitutive expression of abiotic stress-inducible hot pepper CaXTH3, which encodes a xyloglucan endotransglucosylase/hydrolase homolog, improves drought and salt tolerance in transgenic Arabidopsis plants. FEBS letters **580**, 3136-3144.

Clough SJ, Bent AF. 1998. Floral dip: a simplified method for Agrobacterium-mediated

796 transformation of Arabidopsis thaliana. The Plant Journal **16**, 735-743.

797 **Cui F, Brosche M, Lehtonen MT, *et al***. 2016. Dissecting Abscisic Acid Signaling Pathways Involved
798 in Cuticle Formation. Molecular plant **9**, 926-938.

799 **Dai X, Xu Y, Ma Q, Xu W, Wang T, Xue Y, Chong K**. 2007. Overexpression of an R1R2R3 MYB
800 gene, OsMYB3R-2, increases tolerance to freezing, drought, and salt stress in transgenic Arabidopsis.
801 Plant Physiology **143**, 1739-1751.

802 **Danquah A, de Zelicourt A, Colcombet J, Hirt H**. 2014. The role of ABA and MAPK signaling
803 pathways in plant abiotic stress responses. Biotechnol Adv **32**, 40-52.

804 **Denekamp M, Smeekens SC**. 2003. Integration of wounding and osmotic stress signals determines the
805 expression of the AtMYB102 transcription factor gene. Plant Physiology **132**, 1415-1423.

806 **Deng W, Wang Y, Liu Z, Cheng H, Xue Y**. 2014. HemI: a toolkit for illustrating heatmaps. PLoS One
807 **9**, e111988.

808 **Ezer D, Shepherd SJK, Brestovitsky A, *et al***. 2017. The G-Box Transcriptional Regulatory Code in
809 Arabidopsis. Plant Physiology **175**, 628-640.

810 **Fang LC, Su LY, Sun XM, *et al***. 2016. Expression of Vitis amurensis NAC26 in Arabidopsis enhances
811 drought tolerance by modulating jasmonic acid synthesis. Journal of Experimental Botany **67,**
812 2829-2845.

813 **Ferreira RB, Monteiro SS, Picarra-Pereira MA, Teixeira AR**. 2004. Engineering grapevine for
814 increased resistance to fungal pathogens without compromising wine stability. Trends Biotechnol **22,**
815 168-173.

816 **Finkelstein RR, Gampala SSL, Rock CD**. 2002. Abscisic acid signaling in seeds and seedlings. The
817 Plant Cell **14**, S15-S45.

818 **Foster R, Izawa T, Chua NH**. 1994. Plant bZIP proteins gather at ACGT elements. FASEB journal :
819 official publication of the Federation of American Societies for Experimental Biology **8**, 192-200.

820 **Fujii H, Zhu JK**. 2009. Arabidopsis mutant deficient in 3 abscisic acid-activated protein kinases
821 reveals critical roles in growth, reproduction, and stress. Proceedings of the National Academy of
822 Sciences of the United States of America **106**, 8380-8385.

823 **Fujita M, Fujita Y, Maruyama K, *et al***. 2004. A dehydration-induced NAC protein, RD26, is
824 involved in a novel ABA-dependent stress-signaling pathway. The Plant journal : for cell and molecular
825 biology **39**, 863-876.

826 **Fujita Y, Fujita M, Satoh R, *et al***. 2005. AREB1 is a transcription activator of novel
827 ABRE-dependent ABA signaling that enhances drought stress tolerance in Arabidopsis. The Plant Cell
828 **17**, 3470-3488.

829 **Fujita Y, Nakashima K, Yoshida T, *et al***. 2009. Three SnRK2 Protein Kinases are the Main Positive
830 Regulators of Abscisic Acid Signaling in Response to Water Stress in Arabidopsis. Plant Cell
831 Physiology **50**, 2123-2132.

832 **Furihata T, Maruyama K, Fujita Y, *et al***. 2006. Abscisic acid-dependent multisite phosphorylation
833 regulates the activity of a transcription activator AREB1. Proceedings of the National Academy of
834 Sciences of the United States of America **103**, 1988-1993.

835 **Gao M, Zhang H, Guo C, *et al***. 2014. Evolutionary and Expression Analyses of Basic Zipper
836 Transcription Factors in the Highly Homozygous Model Grape PN40024 (Vitis vinifera L.). Plant
837 Molecular Biology Reporter **32**, 1085-1102.

838 **Gao S, Guo W, Feng W, *et al***. 2016. LTP3 contributes to disease susceptibility in Arabidopsis by
839 enhancing abscisic acid (ABA) biosynthesis. Molecular plant pathology **17**, 412-426.

840 **Gao SQ, Chen M, Xu ZS, *et al***. 2011. The soybean GmbZIP1 transcription factor enhances multiple
841 abiotic stress tolerances in transgenic plants. Plant Molecular Biology **75**, 537-553.

842 **Garcia ME, Lynch T, Peeters J, Snowden C, Finkelstein R**. 2008. A small plant-specific protein
843 family of ABI five binding proteins (AFPs) regulates stress response in germinating Arabidopsis seeds
844 and seedlings. Plant Molecular Biology **67**, 643-658.

845 **Gonzalez-Guzman M, Pizzio GA, Antoni R, *et al***. 2012. Arabidopsis PYR/PYL/RCAR receptors
846 play a major role in quantitative regulation of stomatal aperture and transcriptional response to abscisic
847 acid. The Plant Cell **24**, 2483-2496.

848 **Heyndrickx KS, Vandepoele K**. 2012. Systematic identification of functional plant modules through
849 the integration of complementary data sources. Plant Physiology **159**, 884-901.

850 **Hsieh EJ, Cheng MC, Lin TP**. 2013. Functional characterization of an abiotic stress-inducible
851 transcription factor AtERF53 in Arabidopsis thaliana. Plant Molecular Biology **82**, 223-237.

852 **Hsieh TH, Li CW, Su RC, Cheng CP, Sanjaya, Tsai YC, Chan MT**. 2010. A tomato bZIP
853 transcription factor, SlAREB, is involved in water deficit and salt stress response. Planta **231,**
854 1459-1473.

855 **Huang YC, Niu CY, Yang CR, Jinn TL**. 2016. The Heat Stress Factor HSFA6b Connects ABA

Signaling and ABA-Mediated Heat Responses. Plant Physiology **172**, 1182-1199.

Hwang SM, Kim DW, Woo MS, *et al*. 2014. Functional characterization of Arabidopsis HsfA6a as a heat-shock transcription factor under high salinity and dehydration conditions. Plant, cell and environment **37**, 1202-1222.

Iuchi S, Kobayashi M, Taji T, *et al*. 2001. Regulation of drought tolerance by gene manipulation of 9-cis-epoxycarotenoid dioxygenase, a key enzyme in abscisic acid biosynthesis in Arabidopsis. The Plant journal : for cell and molecular biology **27**, 325-333.

Jakoby M, Weisshaar B, Droge-Laser W, *et al*. 2002. bZIP transcription factors in Arabidopsis. Trends in Plant Science **7**, 106-111.

Ji X, Liu G, Liu Y, Zheng L, Nie X, Wang Y. 2013. The bZIP protein from Tamarix hispida, ThbZIP1, is ACGT elements binding factor that enhances abiotic stress signaling in transgenic Arabidopsis. BMC plant biology **13**, 151.

Ji X, Liu G, Liu Y, Nie X, Zheng L, Wang Y. 2015. The regulatory network of ThbZIP1 in response to abscisic acid treatment. Frontiers in Plant Science **6**, 25.

Kagaya Y, Hobo T, Murata M, Ban A, Hattori T. 2002. Abscisic acid-induced transcription is mediated by phosphorylation of an abscisic acid response element binding factor, TRAB1. The Plant Cell **14**, 3177-3189.

Kang JY, Choi HI, Im MY, Kim SY. 2002. Arabidopsis basic leucine zipper proteins that mediate stress-responsive abscisic acid signaling. The Plant Cell **14**, 343-357.

Kim D, Pertea G, Trapnell C, Pimentel H, Kelley R, Salzberg SL. 2013. TopHat2: accurate alignment of transcriptomes in the presence of insertions, deletions and gene fusions. Genome biology **14**, R36.

Kim S, Kang JY, Cho DI, Park JH, Kim SY. 2004. ABF2, an ABRE-binding bZIP factor, is an essential component of glucose signaling and its overexpression affects multiple stress tolerance. The Plant Journal **40**, 75-87.

Kim SY, Ma J, Perret P, Li Z, Thomas TL. 2002. Arabidopsis ABI5 subfamily members have distinct DNA-binding and transcriptional activities. Plant Physiology **130**, 688-697.

Kobayashi F, Maeta E, Terashima A, Kawaura K, Ogihara Y, Takumi S. 2008. Development of abiotic stress tolerance via bZIP-type transcription factor LIP19 in common wheat. Journal of Experimental Botany **59**, 891-905.

Kobayashi Y, Murata M, Minami H, *et al*. 2005. Abscisic acid-activated SNRK2 protein kinases function in the gene-regulation pathway of ABA signal transduction by phosphorylating ABA response element-binding factors. The Plant journal : for cell and molecular biology **44**, 939-949.

Koops P, Pelser S, Ignatz M, Klose C, Marrocco-Selden K, Kretsch T. 2011. EDL3 is an F-box protein involved in the regulation of abscisic acid signalling in Arabidopsis thaliana. Journal of Experimental Botany **62**, 5547-5560.

Kovacs D, Kalmar E, Torok Z, Tompa P. 2008. Chaperone activity of ERD10 and ERD14, two disordered stress-related plant proteins. Plant Physiology **147**, 381-390.

Kumimoto RW, Siriwardana CL, Gayler KK, *et al*. 2013. NUCLEAR FACTOR Y transcription factors have both opposing and additive roles in ABA-mediated seed germination. PLoS One **8**, e59481.

Lata C, Prasad M. 2011. Role of DREBs in regulation of abiotic stress responses in plants. Journal of Experimental Botany **62**, 4731-4748.

Lee SB, Kim HU, Suh MC. 2016a MYB94 and MYB96 Additively Activate Cuticular Wax Biosynthesis in Arabidopsis. Plant Cell Physiology **57**, 2300-2311.

Lee SH, Li CW, Koh KW, Chuang HY, Chen YR, Lin CS, Chan MT. 2014. MSRB7 reverses oxidation of GSTF2/3 to confer tolerance of Arabidopsis thaliana to oxidative stress. Journal of Experimental Botany **65**, 5049-5062.

Lee WJ, Jeong CY, Kwon J, Van Kien V, Lee D, Hong SW, Lee H. 2016b. Drastic anthocyanin increase in response to PAP1 overexpression in fls1 knockout mutant confers enhanced osmotic stress tolerance in Arabidopsis thaliana. Plant Cell Reports **35**, 2369-2379.

Li C, Lv J, Zhao X, *et al*. 2010. TaCHP: a wheat zinc finger protein gene down-regulated by abscisic acid and salinity stress plays a positive role in stress tolerance. Plant Physiology **154**, 211-221.

Li JT, Wang NA, Xin HP, Li SH. 2013. Overexpression of VaCBF4, a transcription factor from Vitis amurensis, improves cold tolerance accompanying increased resistance to drought and salinity in Arabidopsis. Plant Molecular Biology Reporter **31**, 1518-1528.

Li WX, Oono Y, Zhu J, *et al*. 2008. The Arabidopsis NFYA5 transcription factor is regulated transcriptionally and posttranscriptionally to promote drought resistance. The Plant Cell **20**, 2238-2251.

Liao Y, Zou HF, Wei W, *et al*. 2008. Soybean GmbZIP44, GmbZIP62 and GmbZIP78 genes function as negative regulator of ABA signaling and confer salt and freezing tolerance in transgenic Arabidopsis.

916 Planta **228**, 225-240.

917 **Liu C, Mao B, Ou S, *et al***. 2014. OsbZIP71, a bZIP transcription factor, confers salinity and drought
918 tolerance in rice. Plant Molecular Biology **84**, 19-36.

919 **Liu HY, Yang WL, Liu DC, Han YP, Zhang AM, Li SH**. 2011a. Ectopic expression of a grapevine
920 transcription factor VvWRKY11 contributes to osmotic stress tolerance in Arabidopsis. Molecular
921 Biology Reports **38**, 417-427.

922 **Liu WX, Zhang FC, Zhang WZ, Song LF, Wu WH, Chen YF**. 2013. Arabidopsis Di19 functions as
923 a transcription factor and modulates PR1, PR2, and PR5 expression in response to drought stress.
924 Molecular plant **6**, 1487-1502.

925 **Liu YC, Wu YR, Huang XH, Sun J, Xie Q**. 2011b. AtPUB19, a U-box E3 ubiquitin ligase, negatively
926 regulates abscisic acid and drought responses in Arabidopsis thaliana. Molecular plant **4**, 938-946.

927 **Lucinski R, Jackowski G**. 2013. AtFtsH heterocomplex-mediated degradation of apoproteins of the
928 major light harvesting complex of photosystem II (LHCII) in response to stresses. J Plant Physiol **170**,
929 1082-1089.

930 **Ma Y, Szostkiewicz I, Korte A, Moes D, Yang Y, Christmann A, Grill E**. 2009. Regulators of PP2C
931 Phosphatase Activity Function as Abscisic Acid Sensors. Science **324**, 1064-1068.

932 **Martinez F, Arif A, Nebauer SG, *et al***. 2015. A fungal transcription factor gene is expressed in plants
933 from its own promoter and improves drought tolerance. Planta **242**, 39-52.

934 **Merlot S, Gosti F, Guerrier D, Vavasseur A, Giraudat J**. 2001. The ABI1 and ABI2 protein
935 phosphatases 2C act in a negative feedback regulatory loop of the abscisic acid signalling pathway. The
936 Plant journal : for cell and molecular biology **25**, 295-303.

937 **Mitsuda N, Ohme-Takagi M**. 2009. Functional analysis of transcription factors in Arabidopsis. Plant
938 Cell Physiology **50**, 1232-1248.

939 **Moon SJ, Han SY, Kim DY, *et al***. 2015. Ectopic expression of a hot pepper bZIP-like transcription
940 factor in potato enhances drought tolerance without decreasing tuber yield. Plant Molecular Biology **89**,
941 421-431.

942 **Muniz Garcia MN, Giammaria V, Grandellis C, Tellez-Inon MT, Ulloa RM, Capiati DA**. 2012.
943 Characterization of StABF1, a stress-responsive bZIP transcription factor from Solanum tuberosum L.
944 that is phosphorylated by StCDPK2 in vitro. Planta **235**, 761-778.

945 **Nakashima K, Fujita Y, Kanamori N, *et al***. 2009. Three Arabidopsis SnRK2 Protein Kinases,

946 SRK2D/SnRK2.2, SRK2E/SnRK2.6/OST1 and SRK2I/SnRK2.3, Involved in ABA Signaling are
947 Essential for the Control of Seed Development and Dormancy. Plant Cell Physiology **50**, 1345-1363.
948 **Nambara E, Kuchitsu K**. 2011. Opening a new era of ABA research. J Plant Res **124**, 431-435.
949 **Neill S, Desikan R, Hancock J**. 2002. Hydrogen peroxide signalling. Curr Opin Plant Biol **5**, 388-395.
950 **Nelson DE, Repetti PP, Adams TR, *et al***. 2007. Plant nuclear factor Y (NF-Y) B subunits confer
951 drought tolerance and lead to improved corn yields on water-limited acres. Proceedings of the National
952 Academy of Sciences of the United States of America **104**, 16450-16455.
953 **Nicolas P, Lecourieux D, Kappel C, Cluzet S, Cramer G, Delrot S, Lecourieux F**. 2014. The basic
954 leucine zipper transcription factor ABSCISIC ACID RESPONSE ELEMENT-BINDING FACTOR2 is
955 an important transcriptional regulator of abscisic acid-dependent grape berry ripening processes. Plant
956 Physiology **164**, 365-383.
957 **Orellana S, Yanez M, Espinoza A, Verdugo I, Gonzalez E, Ruiz-Lara S, Casaretto JA**. 2010. The
958 transcription factor SlAREB1 confers drought, salt stress tolerance and regulates biotic and abiotic
959 stress-related genes in tomato. Plant, cell and environment **33**, 2191-2208.
960 **Osakabe Y, Mizuno S, Tanaka H, *et al***. 2010. Overproduction of the membrane-bound receptor-like
961 protein kinase 1, RPK1, enhances abiotic stress tolerance in Arabidopsis. The Journal of biological
962 chemistry **285**, 9190-9201.
963 **Park SY, Fung P, Nishimura N, *et al***. 2009. Abscisic Acid Inhibits Type 2C Protein Phosphatases via
964 the PYR/PYL Family of START Proteins. Science **324**, 1068-1071.
965 **Pilati S, Bagagli G, Sonego P, *et al***. 2017. Abscisic Acid Is a Major Regulator of Grape Berry
966 Ripening Onset: New Insights into ABA Signaling Network. Frontiers in Plant Science **8**, 1-16.
967 **Piya S, Kihm C, Rice JH, Baum TJ, Hewezi T**. 2017. Cooperative Regulatory Functions of miR858
968 and MYB83 during Cyst Nematode Parasitism. Plant Physiology **174**, 1897-1912.
969 **Pompelli MF, Martins SC, Antunes WC, Chaves AR, DaMatta FM**. 2010. Photosynthesis and
970 photoprotection in coffee leaves is affected by nitrogen and light availabilities in winter conditions. J
971 Plant Physiol **167**, 1052-1060.
972 **Rai A, Umashankar S, Rai M, Kiat LB, Bing JA, Swarup S**. 2016. Coordinate Regulation of
973 Metabolite Glycosylation and Stress Hormone Biosynthesis by TT8 in Arabidopsis. Plant Physiology
974 **171**, 2499-2515.
975 **Ren X, Chen Z, Liu Y, *et al***. 2010. ABO3, a WRKY transcription factor, mediates plant responses to

abscisic acid and drought tolerance in Arabidopsis. The Plant journal : for cell and molecular biology **63**, 417-429.

Robinson MD, McCarthy DJ, Smyth GK. 2010. edgeR: a Bioconductor package for differential expression analysis of digital gene expression data. Bioinformatics **26**, 139-140.

Rocheta M, Coito JL, Ramos MJ, Carvalho L, Becker JD, Carbonell-Bejerano P, Amancio S. 2016. Transcriptomic comparison between two Vitis vinifera L. varieties (Trincadeira and Touriga Nacional) in abiotic stress conditions. BMC plant biology **16**, 224.

Saez A, Robert N, Maktabi MH, Schroeder JI, Serrano R, Rodriguez PL. 2006. Enhancement of abscisic acid sensitivity and reduction of water consumption in Arabidopsis by combined inactivation of the protein phosphatases type 2C ABI1 and HAB1. Plant Physiology **141**, 1389-1399.

Sakuraba Y, Kim YS, Han SH, Lee BD, Paek NC. 2015. The Arabidopsis Transcription Factor NAC016 Promotes Drought Stress Responses by Repressing AREB1 Transcription through a Trifurcate Feed-Forward Regulatory Loop Involving NAP. The Plant Cell **27**, 1771-1787.

Schweighofer A, Hirt H, Meskiene I. 2004. Plant PP2C phosphatases: emerging functions in stress signaling. Trends in Plant Science **9**, 236-243.

Selvaraj MG, Ishizaki T, Valencia M, *et al*. 2017. Overexpression of an Arabidopsis thaliana galactinol synthase gene improves drought tolerance in transgenic rice and increased grain yield in the field. Plant biotechnology journal **15**, 1465-1477.

Seo PJ, Lee SB, Suh MC, Park MJ, Go YS, Park CM. 2011. The MYB96 transcription factor regulates cuticular wax biosynthesis under drought conditions in Arabidopsis. The Plant Cell **23**, 1138-1152.

Shinozaki K, Yamaguchi-Shinozaki K. 2000. Molecular responses to dehydration and low temperature: differences and cross-talk between two stress signaling pathways. Current Opinion in Plant Biology **3**, 217-223.

Siddiqua M, Nassuth A. 2011. Vitis CBF1 and Vitis CBF4 differ in their effect on Arabidopsis abiotic stress tolerance, development and gene expression. Plant, Cell and Environment **34**, 1345-1359.

Sridha S, Wu K. 2006. Identification of AtHD2C as a novel regulator of abscisic acid responses in Arabidopsis. The Plant journal : for cell and molecular biology **46**, 124-133.

Sun YG, Wang B, Jin SH, Qu XX, Li YJ, Hou BK. 2013. Ectopic expression of Arabidopsis glycosyltransferase UGT85A5 enhances salt stress tolerance in tobacco. PLoS One **8**, e59924.

Tajdel M, Mitula F, Ludwikow A. 2016. Regulation of Arabidopsis MAPKKK18 by ABI1 and SnRK2, components of the ABA signaling pathway. Plant signaling & behavior **11**, e1139277.

Tang N, Zhang H, Li XH, Xiao JH, Xiong LZ. 2012. Constitutive Activation of Transcription Factor OsbZIP46 Improves Drought Tolerance in Rice. Plant Physiology **158**, 1755-1768.

Tian H, Guo H, Dai X, Cheng Y, Zheng K, Wang X, Wang S. 2015. An ABA down-regulated bHLH transcription repressor gene, bHLH129 regulates root elongation and ABA response when overexpressed in Arabidopsis. Scientific reports **5**, 17587.

Tu MX, Wang XH, Huang L, Guo RR, Zhang HJ, Cai JS, Wang XP. 2016a. Expression of a grape bZIP transcription factor, VqbZIP39, in transgenic Arabidopsis thaliana confers tolerance of multiple abiotic stresses. Plant Cell Tissue and Organ Culture **125**, 537-551.

Tu MX, Wang XH, Feng TY, *et al*. 2016b. Expression of a grape (Vitis vinifera) bZIP transcription factor, VIbZIP36, in Arabidopsis thaliana confers tolerance of drought stress during seed germination and seedling establishment. Plant Science **252**, 311-323.

Uno Y, Furihata T, Abe H, Yoshida R, Shinozaki K, Yamaguchi-Shinozaki K. 2000. Arabidopsis basic leucine zipper transcription factors involved in an abscisic acid-dependent signal transduction pathway under drought and high-salinity conditions. Proceedings of the National Academy of Sciences of the United States of America **97**, 11632-11637.

Usadel B, Nagel A, Steinhauser D, *et al*. 2006. PageMan: an interactive ontology tool to generate, display, and annotate overview graphs for profiling experiments. BMC bioinformatics **7**, 535.

Valdes AE, Overnas E, Johansson H, Rada-Iglesias A, Engstrom P. 2012. The homeodomain-leucine zipper (HD-Zip) class I transcription factors ATHB7 and ATHB12 modulate abscisic acid signalling by regulating protein phosphatase 2C and abscisic acid receptor gene activities. Plant Molecular Biology **80**, 405-418.

van Hengel AJ, Roberts K. 2003. AtAGP30, an arabinogalactan-protein in the cell walls of the primary root, plays a role in root regeneration and seed germination. The Plant journal : for cell and molecular biology **36**, 256-270.

Van Leene J, Blomme J, Kulkarni SR, *et al*. 2016. Functional characterization of the Arabidopsis transcription factor bZIP29 reveals its role in leaf and root development. Journal of Experimental Botany **67**, 5825-5840.

Wang J, Li Q, Mao X, Li A, Jing R. 2016. Wheat Transcription Factor TaAREB3 Participates in

Drought and Freezing Tolerances in Arabidopsis. International journal of biological sciences **12**, 257-269.

Wei T, Deng K, Liu D, *et al*. 2016. Ectopic Expression of DREB Transcription Factor, AtDREB1A, Confers Tolerance to Drought in Transgenic Salvia miltiorrhiza. Plant Cell Physiology **57**, 1593-1609.

Wong DCJ, Lopez Gutierrez R, Gambetta GA, Castellarin SD. 2017. Genome-wide analysis of cis-regulatory element structure and discovery of motif-driven gene co-expression networks in grapevine. DNA research : an international journal for rapid publication of reports on genes and genomes **24**, 311-326.

Xiao H, Siddiqua M, Braybrook S, *et al*. 2006. Three grape CBF/DREB1 genes respond to low temperature, drought and abscisic acid. Plant, Cell and Environment **29**, 1410-1421.

Xiong L, Gong Z, Rock CD, *et al*. 2001. Modulation of abscisic acid signal transduction and biosynthesis by an Sm-like protein in Arabidopsis. Developmental cell **1**, 771-781.

Xu R, Wang Y, Zheng H, et al. 2015. Salt-induced transcription factor MYB74 is regulated by the RNA-directed DNA methylation pathway in Arabidopsis. Journal of Experimental Botany **66**, 5997-6008.

Yamaguchi-Shinozaki K, Shinozaki K. 2006. Transcriptional regulatory networks in cellular responses and tolerance to dehydration and cold stresses. In Annual Review of Plant Biology, pp. 781-803.

Yamaguchi-Shinozaki K, Mino M, Mundy J, Chua NH. 1990. Analysis of an ABA-responsive rice gene promoter in transgenic tobacco. Plant Molecular Biology **15**, 905-912.

Yoshida R, Hobo T, Ichimura K, *et al*. 2002. ABA-activated SnRK2 protein kinase is required for dehydration stress signaling in Arabidopsis. Plant Cell Physiology **43**, 1473-1483.

Yoshida T, Fujita Y, Maruyama K, Mogami J, Todaka D, Shinozaki K, Yamaguchi-Shinozaki K. 2015. Four Arabidopsis AREB/ABF transcription factors function predominantly in gene expression downstream of SnRK2 kinases in abscisic acid signalling in response to osmotic stress. Plant, Cell and Environment **38**, 35-49.

Yoshida T, Nishimura N, Kitahata N, *et al*. 2006. ABA-hypersensitive germination3 encodes a protein phosphatase 2C (AtPP2CA) that strongly regulates abscisic acid signaling during germination among Arabidopsis protein phosphatase 2Cs. Plant Physiology **140**, 115-126.

Yoshida T, Fujita Y, Sayama H, *et al*. 2010. AREB1, AREB2, and ABF3 are master transcription

factors that cooperatively regulate ABRE-dependent ABA signaling involved in drought stress tolerance and require ABA for full activation. The Plant Journal **61**, 672-685.

You J, Zong W, Hu H, Li X, Xiao J, Xiong L. 2014. A STRESS-RESPONSIVE NAC1-regulated protein phosphatase gene rice protein phosphatase18 modulates drought and oxidative stress tolerance through abscisic acid-independent reactive oxygen species scavenging in rice. Plant Physiology **166**, 2100-2114.

Yuan YY, Fang LC, Karungo SK, Zhang LL, Gao YY, Li SH, Xin HP. 2016. Overexpression of VaPAT1, a GRAS transcription factor from Vitis amurensis, confers abiotic stress tolerance in Arabidopsis. Plant Cell Reports **35**, 655-666.

Zhang Q, Wang M, Hu J, Wang W, Fu X, Liu JH. 2015. PtrABF of Poncirus trifoliata functions in dehydration tolerance by reducing stomatal density and maintaining reactive oxygen species homeostasis. Journal of Experimental Botany **66**, 5911-5927.

Zhang X, Wollenweber B, Jiang D, Liu F, Zhao J. 2008. Water deficits and heat shock effects on photosynthesis of a transgenic Arabidopsis thaliana constitutively expressing ABP9, a bZIP transcription factor. Journal of Experimental Botany **59**, 839-848.

Zhang X, Wang L, Meng H, Wen HT, Fan YL, Zhao J. 2011. Maize ABP9 enhances tolerance to multiple stresses in transgenic Arabidopsis by modulating ABA signaling and cellular levels of reactive oxygen species. Plant Molecular Biology **75**, 365-378.

Zhu JK. 2002. Salt and drought stress signal transduction in plants. Annual Review of Plant Biology **53**, 247-273.

Zhu ZG, Shi JL, Xu WR, *et al*. 2013. Three ERF transcription factors from Chinese wild grapevine Vitis pseudoreticulata participate in different biotic and abiotic stress-responsive pathways. J Plant Physiol **170**, 923-933.

Zou MJ, Guan YC, Ren HB, Zhang F, Chen F. 2008. A bZIP transcription factor, OsABI5, is involved in rice fertility and stress tolerance. Plant Molecular Biology **66**, 675-683.

1098 **Table 1.** Selected genes involved in abiotic stress with expression changes (FDR<0.05) of at least twofold in the
1099 *VlbZIP30* transgenic plants under different experiments from the microarray.
1100

				Log_2FC (OE / WT)		
Locus	**Symbol**	**Description**	**Reference**	**C**	**M**	**A**
Stress-responsive gene						
AT2G33380	RD20	stress-inducible caleosin	Aubert *et al.*, 2010	-0.421	2.781	2.083
AT5G25610	RD22	responsive to dehydration protein	Yoshida *et al.*, 2002	-0.080	1.160	0.121
AT4G27410	RD26	dehydration-induced NAC protein	Fujita *et al.*, 2004	0.187	1.325	0.560
AT2G42530	COR15B	cold-regulated protein	Nelson *et al.*, 2007	0.329	1.833	1.511
AT2G18050	HIS1-3	dehydration-inducible histone gene	Zhang *et al.*, 2008	0.711	1.106	-0.089
AT5G02020	SIS	involved in salt tolerance	Brinker *et al.*, 2010	0.176	1.530	1.219
AT1G20450	ERD10	early responsive to dehydration	Kovacs *et al.*, 2008	0.217	0.906	1.214
ABA signaling						
AT1G69260	AFP1	ABI five binding protein	Garcia *et al.*, 2008	0.187	1.275	0.646
AT3G29575	AFP3	ABI five binding protein	Garcia *et al.*, 2008	0.286	1.256	0.560
AT4G26080	ABI1	protein phosphatase 2C protein	Merlot *et al.*, 2001	0.186	1.217	-0.060
AT5G57050	ABI2	protein phosphatase 2C protein	Merlot *et al.*, 2001	0.147	1.192	0.303
AT5G59220	HAI1	protein phosphatases 2C protein	Bhaskara *et al.*, 2012	0.219	2.543	1.931
AT1G07430	HAI2	protein phosphatases 2C protein	Bhaskara *et al.*, 2012	0.887	2.247	0.365
AT1G72770	HAB1	protein phosphatases 2C protein	Saez *et al.*, 2006	-0.003	1.255	0.675
AT3G11410	PP2CA	protein phosphatases 2C protein	Yoshida *et al.*, 2006	0.384	1.634	-0.077
AT2G46680	HB7	involved in ABA signaling pathway	Valdes *et al.*, 2012	-0.017	1.555	0.619
AT3G61890	HB12	involved in ABA signaling pathway	Valdes *et al.*, 2012	-0.029	2.007	0.879
AT3G14440	NCED3	key enzyme in ABA biosynthesis	Iuchi *et al.*, 2001	0.833	1.845	0.125
AT1G05100	MAPKKK18	involved in ABA signaling pathway	Tajdel *et al.*, 2016	ND	1.550	1.137
AT2G40330	PYL6	core regulatory component of ABA receptor	Gonzalez-Guzman *et al.*, 2012	-0.342	-1.213	ND
Transcription factor						
AT4G05100	MYB74	R2R3-MYB family gene	Xu *et al.*, 2015	0.275	1.672	0.691
AT4G21440	MYB102	R2R3-MYB family gene	Denekamp and Smeekens, 2003	ND	1.630	0.332
AT4G34000	ABF3	ABRE-binding transcription factor	Kang *et al.*, 2002	0.013	1.129	0.565
AT1G45249	ABF2	ABRE-binding transcription factor	Fujita *et al.*, 2005	0.001	1.954	0.722
AT3G19290	ABF4	ABRE-binding transcription factor	Kang *et al.*, 2002	0.053	1.050	0.473
AT4G25480	DREB1A	DRE-binding transcription factor	Wei *et al.*, 2016	0.286	2.020	-0.402
AT1G54160	NFYA5	CCAAT-binding transcription factor	Li *et al.*, 2008	0.342	1.469	0.367
AT5G47640	NFYB2	His-like transcription factor	Kumimoto *et al.*, 2013	0.200	2.885	0.755
AT1G69490	NAP	NAC family transcription factor	Sakuraba *et al.*, 2015	0.377	1.297	0.867
AT4G09820	TT8	bHLH transcription factor	Rai *et al.*, 2016	-0.591	1.963	0.201
AT4G18170	WRKY28	WRKY transcription factor	Babitha *et al.*, 2013	-0.577	1.277	0.594
AT2G20880	ERF053	ethylene response factor	Hsieh *et al.*, 2013	ND	ND	3.986
AT2G43140	BHLH129	bHLH transcription factor	Tian *et al.*, 2015	-0.21	-1.005	ND
AT3G23250	MYB15	R2R3-MYB family gene	Li *et al.*, 2010	-0.098	-1.527	-0.437
Disease						

AT5G59310	LTP4	susceptibility to pseudomonas	Gao *et al*., 2016	0.198	1.467	0.086
AT1G75040	PR5	pathogenesis-related gene	Liu *et al*., 2013	-0.542	2.521	ND
AT1G54040	ESP	involved in necrotrophic fungi resistance	Buxdorf *et al*., 2013	ND	2.064	1.439
Hsp						
AT3G22830	HSFA6B	heat stress transcription factor	Huang *et al*., 2016	0.129	1.648	0.465
AT5G43840	HSFA6A	heat stress transcription factor	Hwang *et al*., 2014	ND	2.398	1.028
Metabolism						
AT2G39800	P5CS1	involved in proline biosynthesis	Martinez *et al*., 2015	0.251	1.798	1.564
AT1G56650	MYB75	involved in anthocyanin metabolism	Lee *et al*., 2016b	ND	1.730	0.606
AT3G63060	EDL3	regulate anthocyanin accumulation	Koops *et al*., 2011	-0.121	1.232	0.026
AT2G05100	LHCB2.1	chlorophyll a/b-binding proteins	Lucinski and Jackowski, 2013	-0.311	1.240	0.651
AT2G05070	LHCB2.2	chlorophyll a/b-binding proteins	Lucinski and Jackowski, 2013	-0.294	1.601	0.818
AT3G27690	LHCB2.4	chlorophyll a/b-binding proteins	Lucinski and Jackowski, 2013	-0.103	1.920	1.153
AT3G47600	MYB94	activate cuticular wax biosynthesis	Lee *et al*., 2016a	0.134	1.913	0.312
AT5G62470	MYB96	activate cuticular wax biosynthesis	Lee *et al*., 2016a	0.241	2.048	0.738
AT2G33790	ATAGP30	arabinogalactan protein	van Hengel and Roberts, 2003	0.543	-0.042	1.253
Transporter						
AT1G22370	AtUGT85A5	UDP-glycosyl transferase	Sun *et al*., 2013	0.051	1.118	0.621
AT4G13420	HAK5	high affinity K^+ transporter	Brauer *et al*., 2016	0.460	0.154	-1.043
AT2G02930	ATGSTF3	glutathione transferase (GST)	Lee *et al*., 2014	-0.316	-0.977	-1.478
Enzyme						
AT1G56600	AtGolS2	galactinol synthase	Selvaraj *et al*., 2017	-0.059	1.157	-0.073
AT1G60190	PUB19	U-Box E3 Ubiquitin Ligase	Liu *et al*., 2011b	-0.059	1.157	-0.073
AT1G69270	RPK1	leucine-rich receptor-like kinase	Osakabe *et al*., 2010	0.148	1.057	-0.006

FDR, false discovery rate; FC, fold change; OE / WT, overexpression line / wild type; M, mannitol; A, ABA; ND, not detected

1111 # Figure legends

1112 **Fig. 1.** Multiple sequence alignment. Full-length sequence comparison of VlbZIP30
1113 (VIT_13s0175g00120) with the ABF/DPBF subfamily of group A bZIP proteins from
1114 *Arabidopsis thaliana* (AT) and grapevine (*Vitis vinifera*, VIT). AtABF1 (AT1G49720),
1115 AtABF2 (AT1G45249), AtABF3 (AT4G34000), AtABF4 (AT3G19290), AtDPBF1
1116 (AT2G36270), AtDPBF2 (AT3G44460), AtDPBF3 (AT3G56850), AtDPBF4
1117 (AT2G41070) and VvABF2 (VIT_18s0001g10450) were used for the alignment.
1118 Conserved residues with 100%, 75-99 % or 33-75% amino identity are shaded in
1119 black, dark gray and light gray, respectively. The conserved bZIP domains are
1120 indicated with black rectangles. Putative phosphorylation sites (C1, C2, C3 and C4,
1121 underlined) are marked with asterisks.

1122

1123 **Fig. 2.** Phylogenetic analysis of VlbZIP30 and expression analysis of *VlbZIP30*. (A)
1124 The phylogenetic tree represents VlbZIP30 (black circle) and other bZIP amino acid
1125 sequences from *Arabidopsis thaliana* (AT) and grapevine (*Vitis vinifera*, VIT). The
1126 clustering of the group A bZIP proteins and the other groups of bZIP proteins (group
1127 H, AtHY5; I, AtbZIP29; E, AtbZIP34; L, AtbZIP76; S AtGBF5; B, bZIP28; D
1128 AtTGA6; J, AtbZIP62; K, AtbZIP60; F, AtbZIP19; and C, AtBZO2H2) have
1129 previously beenreported by Jakoby *et al*. (2002) and Nicolas *et al*. (2014). (B)
1130 Expression profiles of *VlbZIP30* in grapevine following abscisic acid (ABA) and
1131 dehydration treatments. Data represent the mean values ±SE from three independent
1132 experiments. Asterisks indicate statistical significance (*$0.01 < P < 0.05$, **$P < 0.01$,
1133 Student's *t*-test) between the treated and untreated control plants. (C) Patterns of
1134 *VlbZIP30* promoter-driven GUS (β-glucosidase) expression in *A. thaliana* at different
1135 growth stages. Mature embryos cultivated on Murashige-Skoog (MS) agar medium
1136 (a), or MS agar medium supplemented with 300 mM mannitol (b) or 0.5 μM ABA (c)
1137 for 2 d. Scale bar = 500 μm. Seven-day-old seedlings cultivated on MS agar medium
1138 (d), or MS agar medium supplemented with 300 mM mannitol (e) or 0.5 μM ABA (f)
1139 for 7 d. Scale bar = 500 μm. Fourteen-day-old seedlings transferred from MS medium

plates into MS agar medium (g) or MS agar medium supplemented with 300 mM mannitol (h) or 100 μM ABA (i) for 7 d. Scale bar = 2 mm. (j) 3-week-old plant. (k) 3-week-old plant after dehydration for 2 h. (l) Guard cells of 3-week-old plant. Scale bar = 50 μm. (m) Guard cells of 3-week-old plant after dehydration for 2 h. Scale bar = 50 μm. (n) Inflorescence. Scale bar = 2 mm. (o) Leaf. Scale bar = 200 μm. (p) Flower. Scale bar = 200 μm. (q) Silique. Scale bar = 2 mm.

Fig. 3. Phenotypes of wild type (WT) and *VlbZIP30* overexpressing (OE) transgenic lines at the greening cotyledon stage following mannitol and abscisic acid (ABA) treatments. (A) Greening cotyledons from WT and transgenic lines 7 d after seeds were cultivated on Murashige-Skoog (MS) agar medium, with or without 300 mM or 350 mM mannitol, or 0.5 μM or 1 μM ABA. (B) Cotyledon greening rates of WT and transgenic lines 7 d after cultivation on MS agar medium with or without 300 mM or 350 mM mannitol, or 0.5 μM or 1 μM ABA. (C) and (D) Cotyledon greening rates of WT and transgenic lines grown on MS basal medium containing 350 mM mannitol (C) or 1 μM ABA (D). (E) Endogenous ABA levels of WT and transgenic lines 7 d after cultivationon MS agar medium, or MS agar medium containing 350 mM mannitol or 1μM ABA. Three independent experiments were performed with ~100 seeds per experiment. Error bars indicate ±SE. Asterisks indicate statistical significance (*0.01 < P < 0.05, **P < 0.01, Student's *t*-test) between the transgenic and WT plants.

Fig. 4. Phenotypes of wild type (WT) and *VlbZIP30*-overexpressing (OE) transgenic lines at the post-germination growth stage during mannitol and abscisic acid (ABA) treatments. (A) Photographs of morphology in WT and transgenic lines 14 d after seeds were cultivated on Murashige-Skoog (MS) agar medium with or without 300 mM mannitol or 0.5 μM ABA. (B) Root length of WT and transgenic lines after 7 d of growth with or without mannitol (300 mM or 350 mM) or ABA (50 μM or 100 μM). (C) Photographs of 14-day-old seedlings transferred from MS agar medium to MS agar medium or MS agar medium supplemented with mannitol (300 mM or 350 mM) or ABA (50 μM or 100 μM) for 7 d. Electrolyte leakage (D) and malondialdehyde

(MDA) content (E) of 14-day-old seedlings transferred from MS agar medium to MS agar medium or MS agar medium supplemented with mannitol (300 mM or 350 mM) or ABA (50 μM or 100 μM) for 7 d. In all cases, data represent mean values ±SE from three independent experiments. Asterisks indicate statistical significance (*0.01 < P < 0.05, **P < 0.01, Student's *t*-test) between the transgenic and WT plants.

Fig. 5. Venn diagram representation of the differentially expressed genes (DEGs) in four comparisons of wild type (WT) and *VlbZIP30*-overexpressing plants (OE) grown under control conditions, abscisic acid (ABA) or mannitol stress. (A) Experimental set up: WT and OE transgenic seeds were cultivated on Murashige-Skoog (MS) agar medium (WTC, OEC) or MS agar medium supplemented with 0.5 μM ABA (WTA, OEA) or 300 mM mannitol (WTM, OEM) for 7 d. (B) and (C) show the numbers of overlapping down-regulated and up-regulated genes, respectively. The numbers in brackets represent the total numbers of DEGs in different comparisons. The DEGs in red circles were selected for further analysis. (D) The selected up-regulated genes in the comparisons (OE / WT) under control conditions, ABA or mannitol stress in *Arabidopsis thaliana*. (E) The grapevine (*Vitis vinifera*) homologs of the selected *A. thaliana* DEGs from (D).

Fig. 6. Gene ontology (GO) analyses of the differentially expressed genes (DEGs) in the *VlbZIP30*-overexpressing plants (OE) compared with wild type (WT) plants in response to abscisic acid (ABA) (OEA / WTA) or mannitol stress (OEM / WTM). Bar graphs separately display the numbers of DEGs classified into each GO category among the genes up- or down-regulated in the comparisons (OE / WT) induced by ABA, mannitol, or ABA and mannitol treatment. GO analyses are based on the PageMan profiling tool (Usadel *et al.*, 2006) and the Arabidopsis Functional Modules Supporting Data (Heyndrickx and Vandepoele, 2012).

Fig. 7. Experimental validation of transcriptome data by expression analysis of representative drought-responsive genes in *Arabidopsis thaliana* using qRT-PCR. The

1200 expression level in the wild type (WT) plants under control conditions was defined as
1201 1.0. The *AtActin2* gene was used as an internal control. Data represent mean values
1202 ±SE from three independent experiments. Asterisks indicate statistical significance
1203 (*0.01 < P < 0.05, **P < 0.01, Student's *t*-test) between the overexpressing (OE) lines
1204 and WT plants.
1205
1206 **Fig. 8.** Enrichment of a potential G-box motif in *VlbZIP30* induced genes. (A) and (B)
1207 DREME motif analysis, showing the predicted G-box (ACGTGKV) motif (A) in the
1208 promoter regions of selected *Arabidopsis thaliana* up-regulated genes from the
1209 overexpressing (OE) lines, and the potential G/C-box (MCACGTS) motif (B) in the
1210 promoter regions of the corresponding grapevine (*Vitis vinifera*) homologs. (C) and
1211 (D) Number of predicted G-box motifs in the promoters of the selected *A. thaliana*
1212 genes (C), and the number of predicted G/C-box motifs in the promoter of the
1213 corresponding grapevine homologs (D). Predicted *VlbZIP30*-induced *A. thaliana* and
1214 grapevine genes with at least three G-box or G/C-box motifs were selected for further
1215 analyses (highlighted in blue). (E) and (F) Frequency of the predicted G-box motif in
1216 the promoters of the selected *A. thaliana* genes with respect to their distance from the
1217 start codon site (E), and the frequency of the potential G/C-box motif in the promoters
1218 of the corresponding grapevine homologs with respect to their distance from the start
1219 codon site (F).
1220
1221 **Fig. 9.** *In silico* promoter analyses of the selected *Arabidopsis thaliana* genes and the
1222 grapevine (*Vitis vinifera*) homologs. (A) Venn diagram showing the selected *A.*
1223 *thaliana* genes with 3 or more predicted G-box elements and the *A. thaliana*
1224 homologs of selected grapevine genes with 3 or more predicted G-box motifs. (C)
1225 Venn diagrams of the selected grapevine genes with 3 or more predicted G-box motifs
1226 and the grapevine homologs of the selected *A. thaliana* genes with 3 or more
1227 predicted G-box motifs. (B) and (D) The 1,500 bp promoter regions of the
1228 overlapping 39 *A. thaliana* genes from (A) and 35 grapevine genes from (C) were
1229 analyzed using the DREME motif enrichment tool. The potential *A. thaliana* G-box

and grapevine G-box motif enrichments were identified using the whole genome sequences from *A. thaliana* and grapevine as a reference.

Fig. 10. The expression profiles of predicted *VlbZIP30* induced genes in grapevine (*Vitis vinifera*) following abscisic acid (ABA) or drought treatment. (A) Venn diagram of the selected up-regulated genes in two different grapevine-related databases (for ABA; Pilati *et al*., 2017 and for drought stress; Rocheta *et al*., 2016) with the 35 predicted grapevine genes. Thirty-one and 25 predicted grapevine genes were present in the RNA-seq and GeneChips® data. The numbers in brackets represent the numbers of up-regulated genes in the two different grapevine-related databases. (B) Heat maps showing the expression of the 27 genes found in (A). RNA-seq analysis was performed of transcripts expressed in the skin of berries from grapevines treated, or not, with ABA for 20 h and 44 h. The GrapeGene GeneChips® data was derived from an analysis of the leaves of two *V. vinifera* L. varieties (Trincadeira, TR and Touriga Nacional, TN) grown under control and drought conditions in a greenhouse, as well as under fully irrigated and non-irrigated conditions in the field. Heat map color gradation in red indicates the increase in expression (log2 fold change). (C) Gene expression profiles of randomly selected *VlbZIP30*-induced grapevine candidate genes analyzed using qRT-PCR. For each gene, the expression level in the 0 h sample from the ABA and dehydration treatments was defined as 1.0. The *VvActin1* gene was used as an internal control. Data represent mean values ±SE from three independent experiments. Asterisks indicate statistical significance (*$0.01 < P < 0.05$, **$P < 0.01$, Student's *t*-test) between the treated and untreated control plants.

Fig. 11. *VlbZIP30*-overexpressing *Arabidopsis thaliana* show enhanced dehydration tolerance at the adult stage. (A) Drought tolerance phenotypes and survival rates of wild type (WT) and transgenic (OE) lines grown in soil. Three-week-old plants (upper panel) were dehydrated for 8 d (middle panel) and then rehydrated for 3 d (lower panel). DDT: day of drought treatment. (B) Leaf phenotype of 3-week-old WT and

OE lines before and after dehydration for 1, 2, 3 h. Staining with trypan blue of leaves detached from WT and OE lines and left to dehydrate for 3 h. (C) Relative water loss rates in WT and OE lines during 3 h of dehydration. (D) Endogenous abscisic acid (ABA) levels of WT and OE lines before and after dehydration for 1 h and 2 h. (E) Expression profiles of stress-related genes in WT and OE analyzed using qRT-PCR. Expression levels were based on total RNA extracted from the aerial parts of 3-week-old WT and OE lines that had been dehydrated on dry filter paper for 0, 1, 2 h. The *AtActin2* gene was used as an internal control. In all cases, data represent mean values ±SE from three independent experiments. Asterisks indicate statistical significance (*$0.01 < P < 0.05$, **$P < 0.01$, Student's *t*-test) between the OE and WT plants.

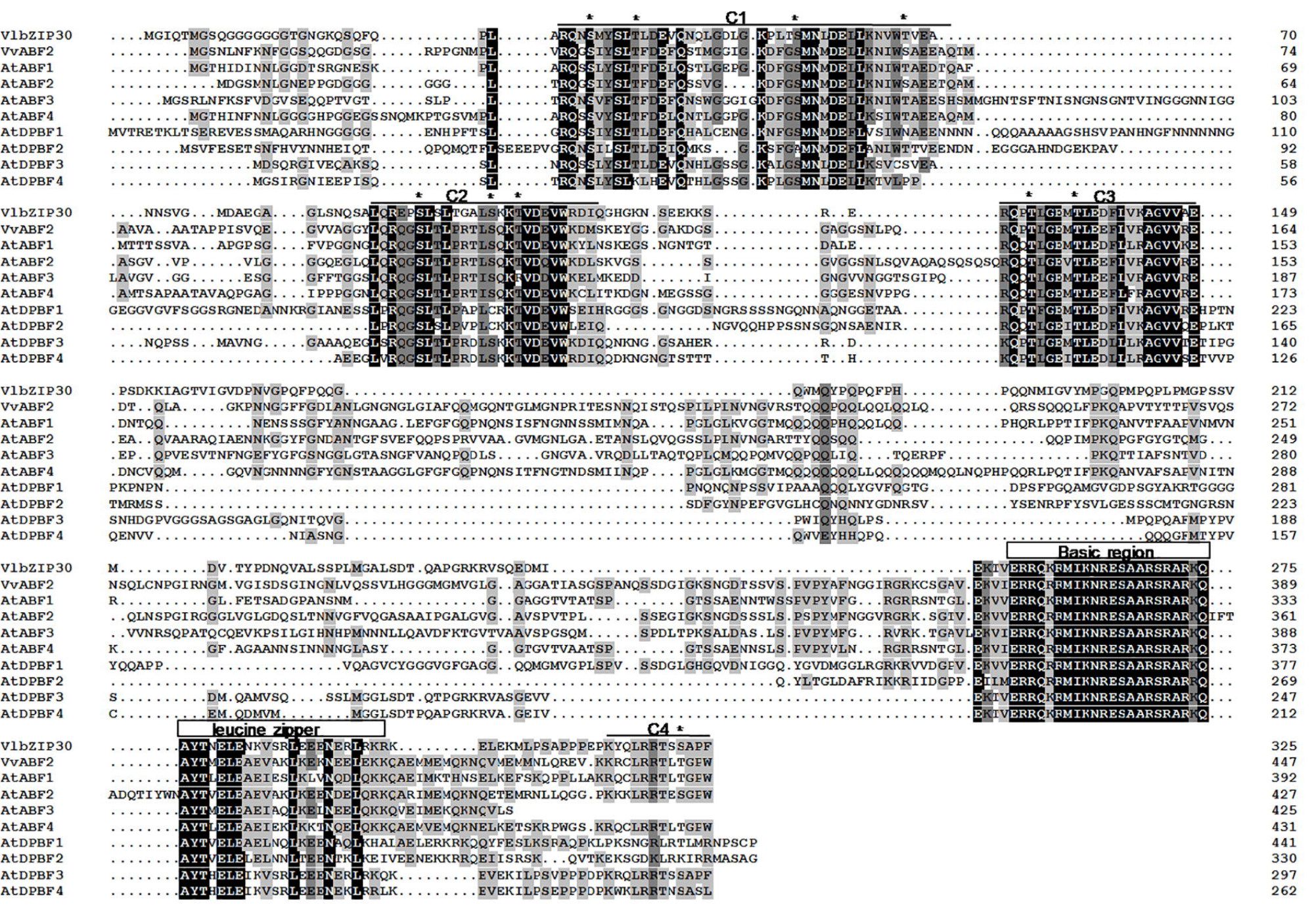
C1
C2
C3
C4
Basic region
leucine zipper
VlbZIP30
VvABF2
AtABF1
AtABF2
AtABF3
AtABF4
AtDPBF1
AtDPBF2
AtDPBF3
AtDPBF4

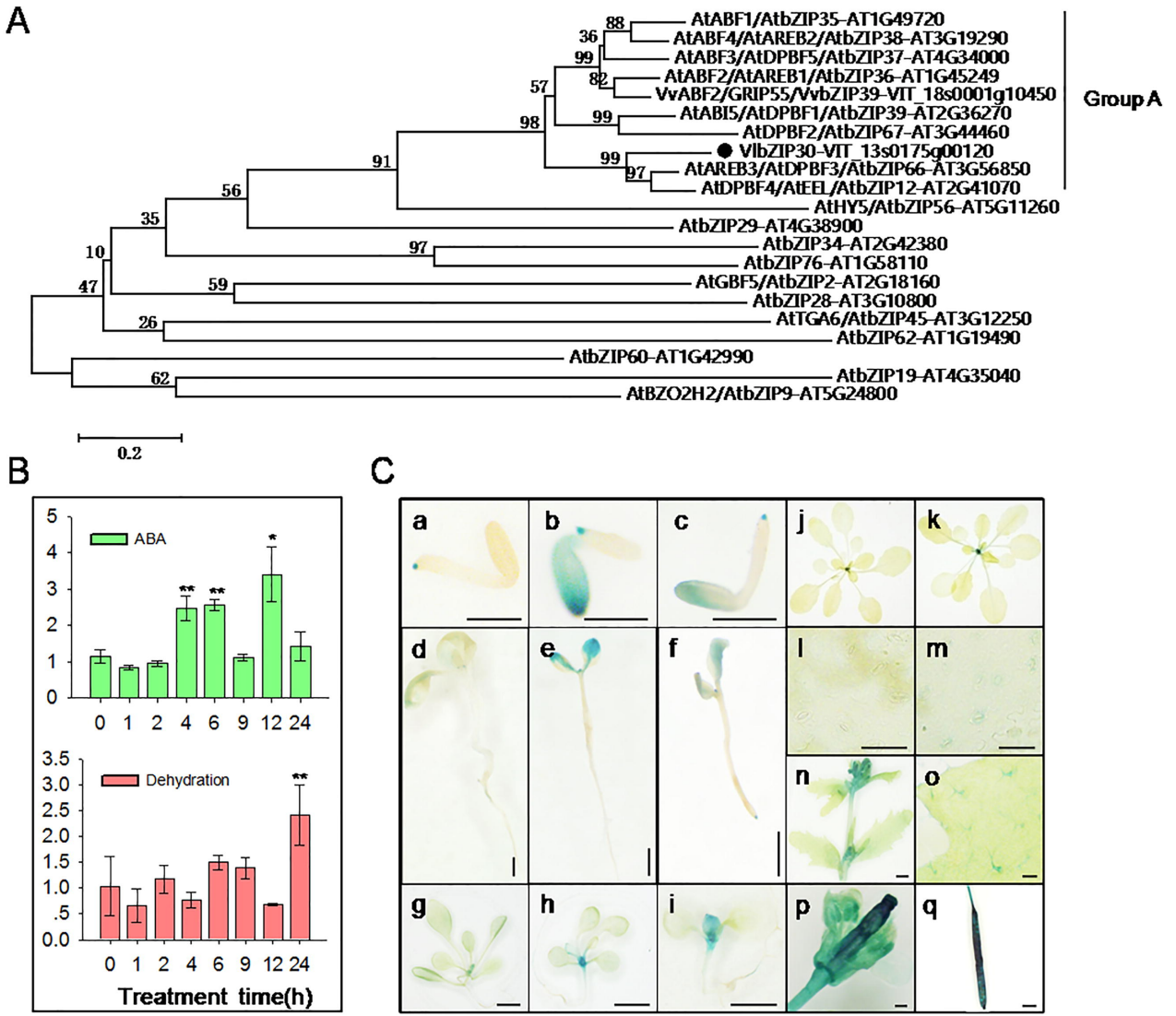
A
AtABF1/AtbZIP35-AT1G49720
AtABF4/AtAREB2/AtbZIP38-AT3G19290
AtABF3/AtDPBF5/AtbZIP37-AT4G34000
AtABF2/AtAREB1/AtbZIP36-AT1G45249
VvABF2/GRIP55/VvbZIP39-VIT_18s0001g10450
AtABI5/AtDPBF1/AtbZIP39-AT2G36270
AtDPBF2/AtbZIP67-AT3G44460
VlbZIP30-VIT_13s0175g00120
AtAREB3/AtDPBF3/AtbZIP66-AT3G56850
AtDPBF4/AtEEL/AtbZIP12-AT2G41070
AtHY5/AtbZIP56-AT5G11260
AtbZIP29-AT4G38900
AtbZIP34-AT2G42380
AtbZIP76-AT1G58110
AtGBF5/AtbZIP2-AT2G18160
AtbZIP28-AT3G10800
AtTGA6/AtbZIP45-AT3G12250
AtbZIP62-AT1G19490
AtbZIP60-AT1G42990
AtbZIP19-AT4G35040
AtBZO2H2/AtbZIP9-AT5G24800
Group A
0.2
B
ABA
Dehydration
Treatment time(h)
C

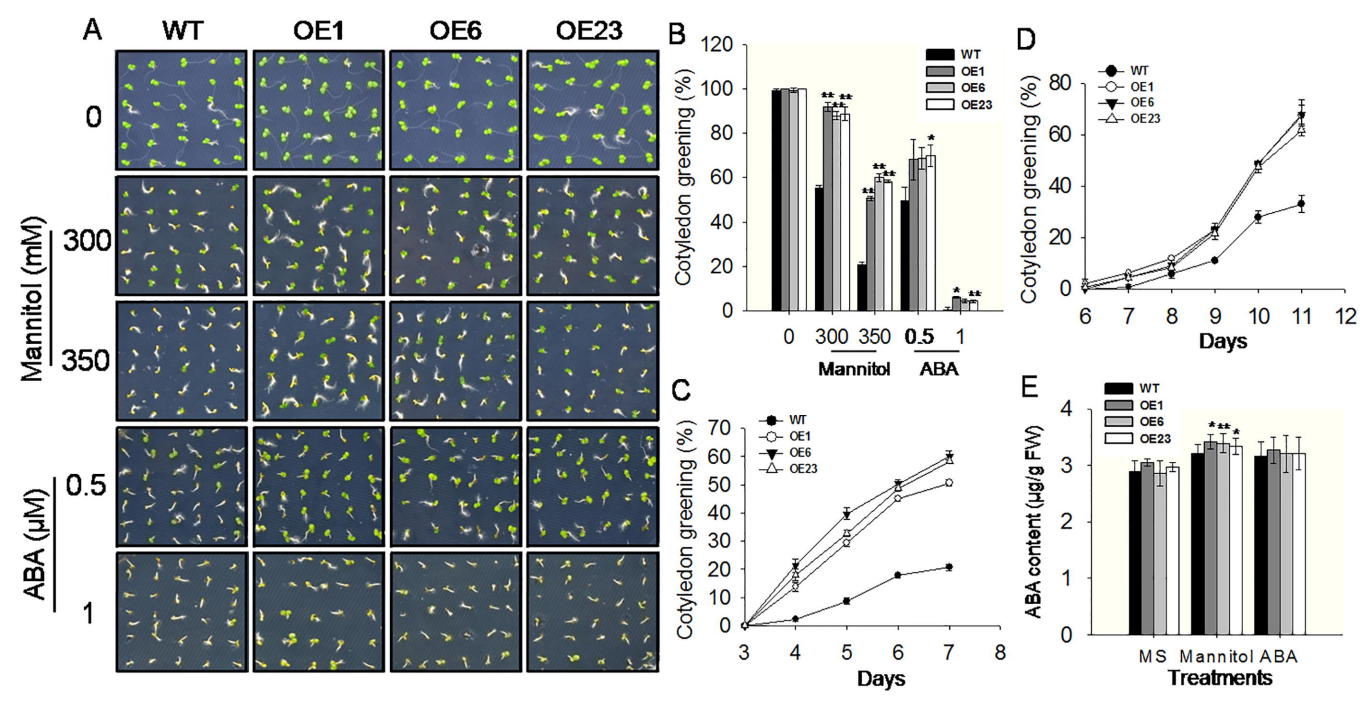
A
WT
OE1
OE6
OE23
0
300
350
Mannitol (mM)
0.5
1
ABA (μM)
B
Cotyledon greening (%)
WT
OE1
OE6
OE23
0
300
350
0.5
1
Mannitol
ABA
C
Cotyledon greening (%)
Days
D
Cotyledon greening (%)
Days
E
ABA content (μg/g FW)
MS
Mannitol
ABA
Treatments

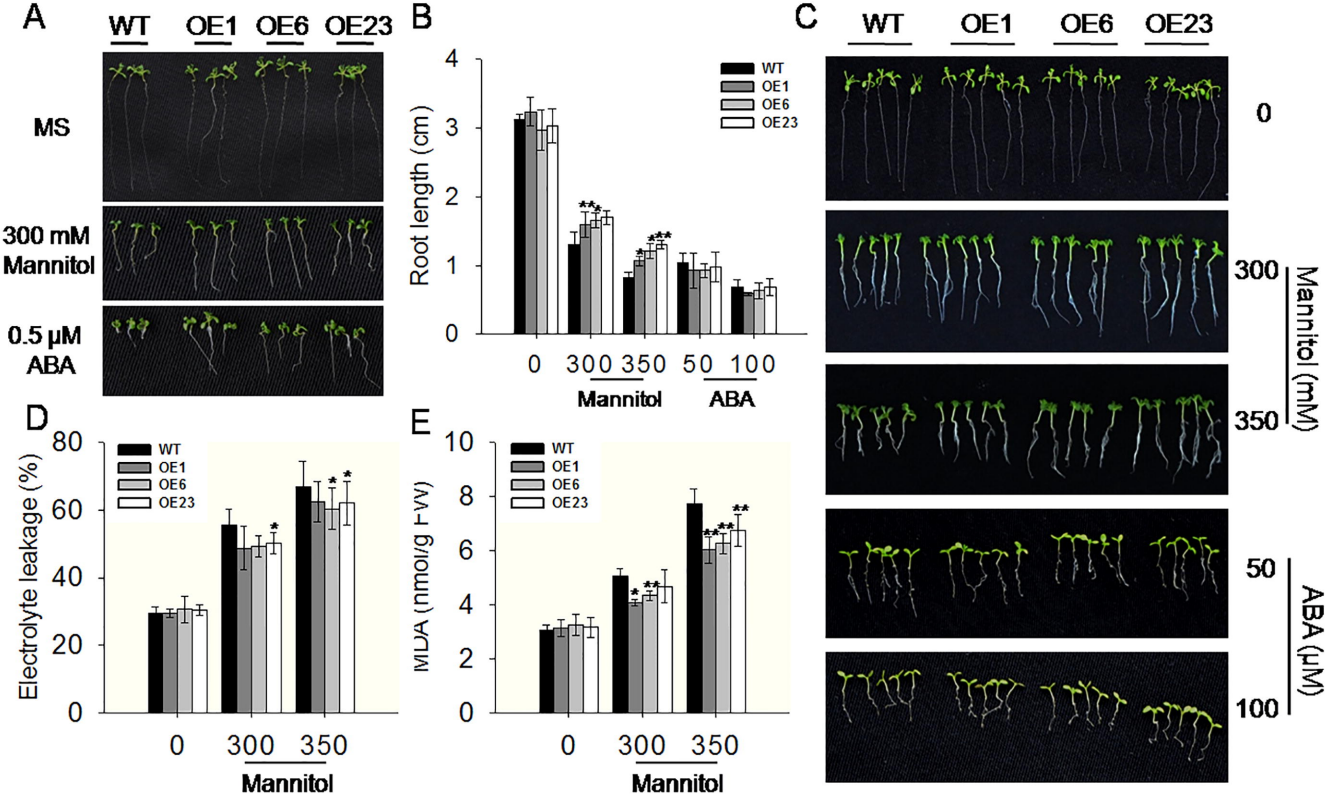
A
WT
OE1
OE6
OE23
MS
300 mM Mannitol
0.5 μM ABA
B
Root length (cm)
WT
OE1
OE6
OE23
0
300
350
50
100
Mannitol
ABA
C
WT
OE1
OE6
OE23
0
300
350
Mannitol (mM)
50
100
ABA (μM)
D
Electrolyte leakage (%)
WT
OE1
OE6
OE23
0
300
350
Mannitol
E
MDA (nmol/g FW)
WT
OE1
OE6
OE23
0
300
350
Mannitol

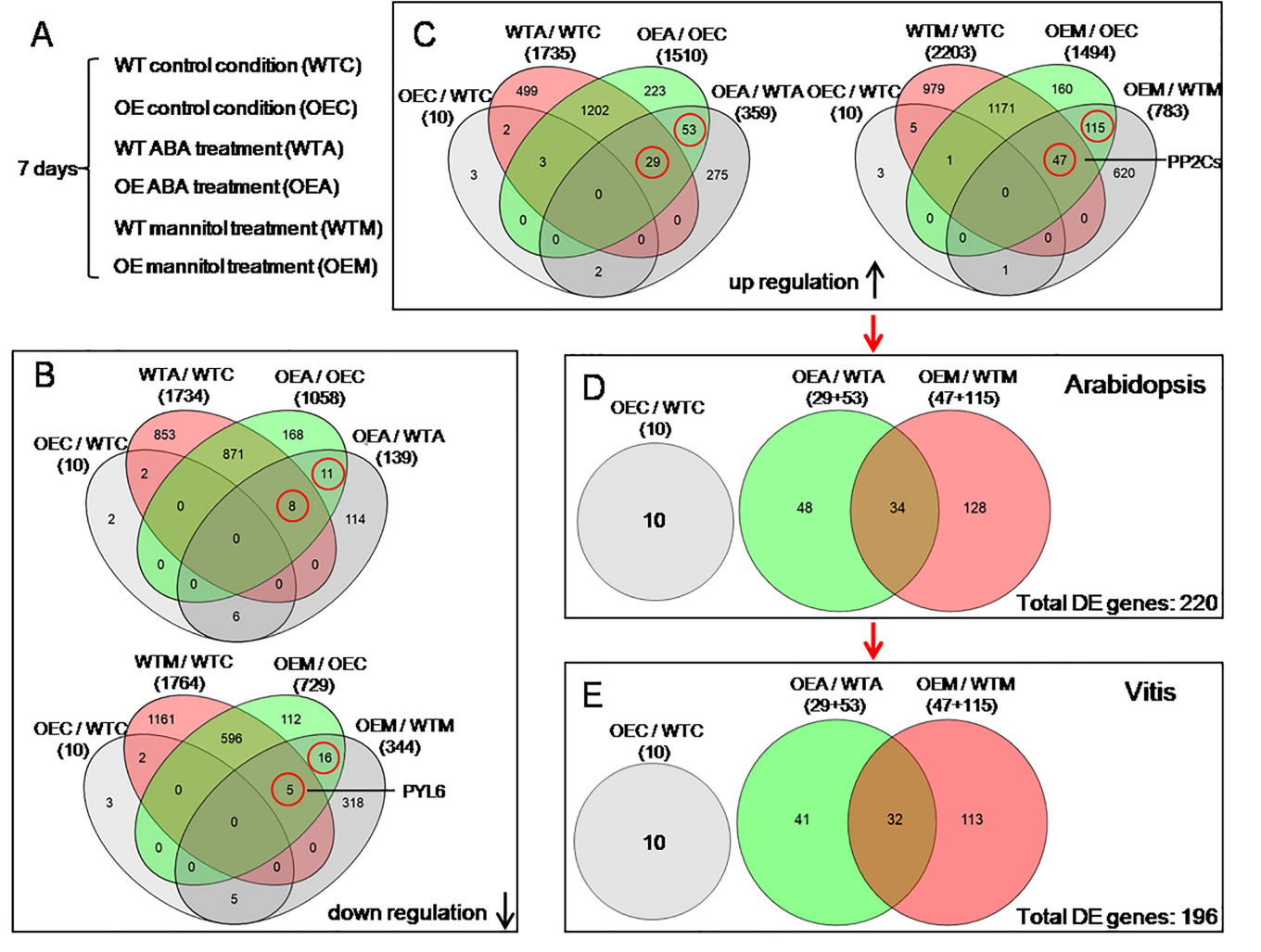
A
7 days
WT control condition (WTC)
OE control condition (OEC)
WT ABA treatment (WTA)
OE ABA treatment (OEA)
WT mannitol treatment (WTM)
OE mannitol treatment (OEM)
C
WTA / WTC (1735)
OEA / OEC (1510)
OEC / WTC (10)
OEA / WTA (359)
499
1202
223
2
53
3
29
275
0
0
0
0
0
2
WTM / WTC (2203)
OEM / OEC (1494)
OEC / WTC (10)
OEM / WTM (783)
979
160
5
1171
115
1
47
PP2Cs
3
620
0
0
0
0
0
1
up regulation
B
WTA / WTC (1734)
OEA / OEC (1058)
OEC / WTC (10)
OEA / WTA (139)
853
168
2
871
11
0
8
2
114
0
0
0
0
0
6
WTM / WTC (1764)
OEM / OEC (729)
OEC / WTC (10)
OEM / WTM (344)
1161
112
2
596
16
0
5
PYL6
3
318
0
0
0
0
0
5
down regulation
D
OEC / WTC (10)
OEA / WTA (29+53)
OEM / WTM (47+115)
Arabidopsis
10
48
34
128
Total DE genes: 220
E
OEC / WTC (10)
OEA / WTA (29+53)
OEM / WTM (47+115)
Vitis
10
41
32
113
Total DE genes: 196

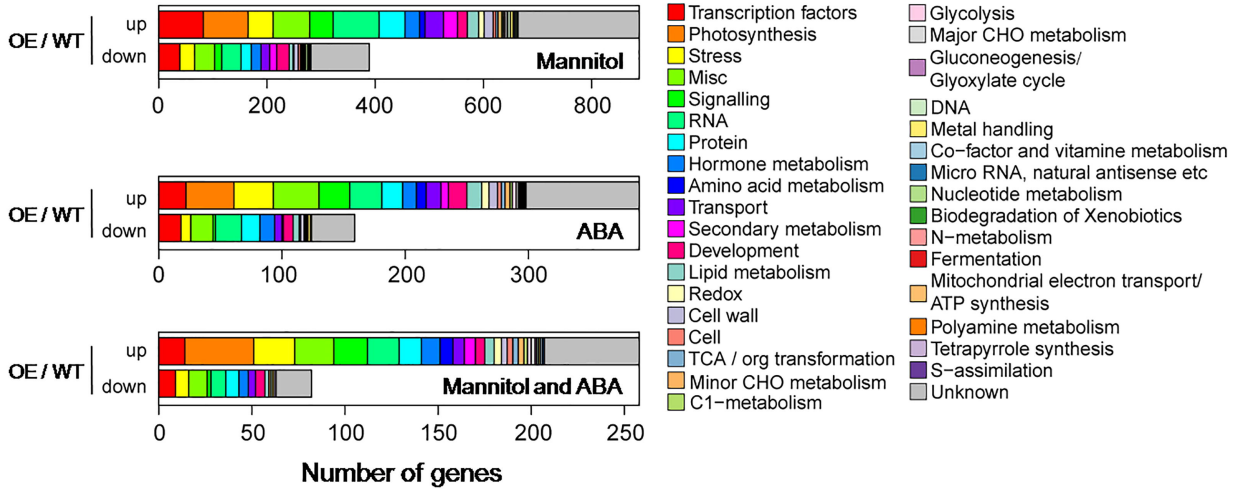
OE / WT
up
down
Mannitol
0
200
400
600
800
OE / WT
up
down
ABA
0
100
200
300
OE / WT
up
down
Mannitol and ABA
0
50
100
150
200
250
Number of genes
Transcription factors
Photosynthesis
Stress
Misc
Signalling
RNA
Protein
Hormone metabolism
Amino acid metabolism
Transport
Secondary metabolism
Development
Lipid metabolism
Redox
Cell wall
Cell
TCA / org transformation
Minor CHO metabolism
C1−metabolism
Glycolysis
Major CHO metabolism
Gluconeogenesis/
Glyoxylate cycle
DNA
Metal handling
Co−factor and vitamine metabolism
Micro RNA, natural antisense etc
Nucleotide metabolism
Biodegradation of Xenobiotics
N−metabolism
Fermentation
Mitochondrial electron transport/
ATP synthesis
Polyamine metabolism
Tetrapyrrole synthesis
S−assimilation
Unknown

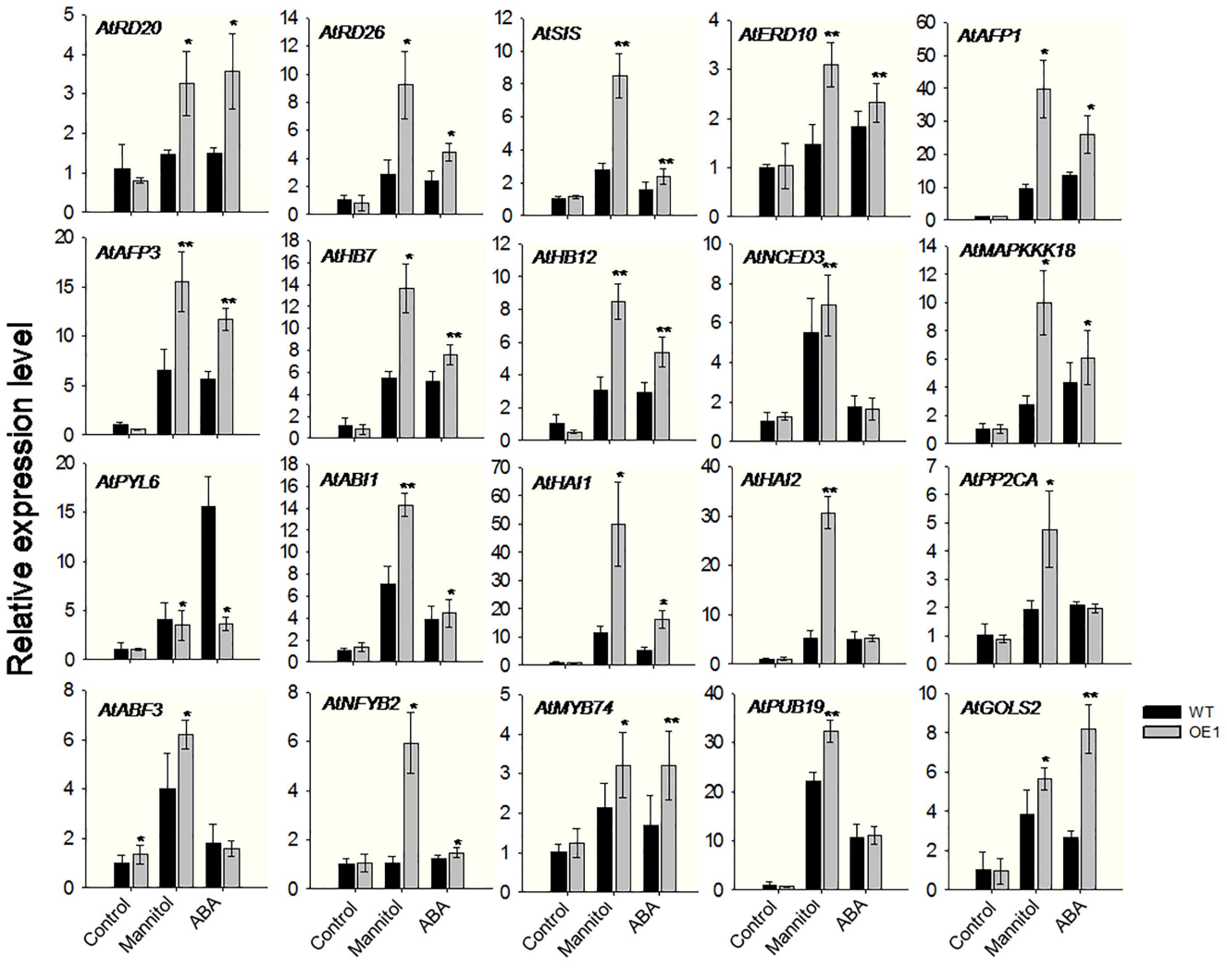
Relative expression level
AtRD20
AtRD26
AtSIS
AtERD10
AtAFP1
AtAFP3
AtHB7
AtHB12
AtNCED3
AtMAPKKK18
AtPYL6
AtABI1
AtHAI1
AtHAI2
AtPP2CA
AtABF3
AtNFYB2
AtMYB74
AtPUB19
AtGOLS2
Control
Mannitol
ABA
WT
OE1

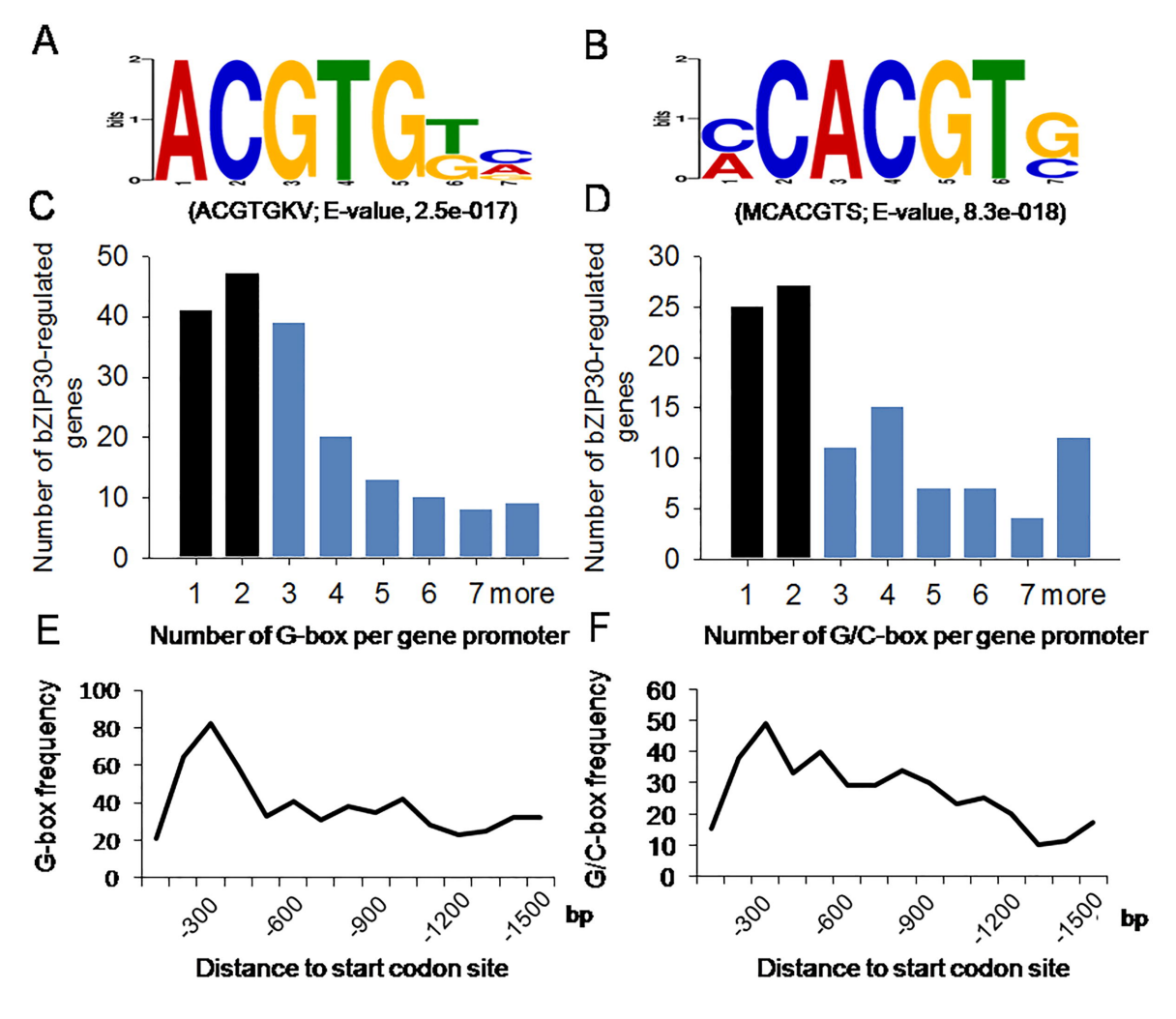
A
B
(ACGTGKV; E-value, 2.5e-017)
(MCACGTS; E-value, 8.3e-018)
C
D
Number of bZIP30-regulated genes
Number of G-box per gene promoter
Number of G/C-box per gene promoter
E
F
G-box frequency
G/C-box frequency
Distance to start codon site
bp

A

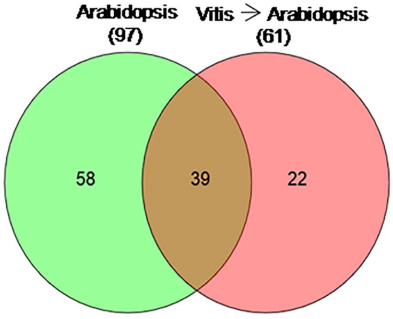

B

	Motif	Logo	E-value	Frequency in the *VlbZIP30* induced genes (%)		Frequency in the genome (%)
				In 39 genes	In 220 genes	
1	CACGTG		9.0e-012	89.7	70.0	51.5
2	DAGAGAGA		1.1e-005	76.9	70.5	69.4
3	AAGAAAAR		7.9e-004	92.3	85.7	80.2
4	ABATATAT		9.9e-004	76.9	66.7	52.6

C

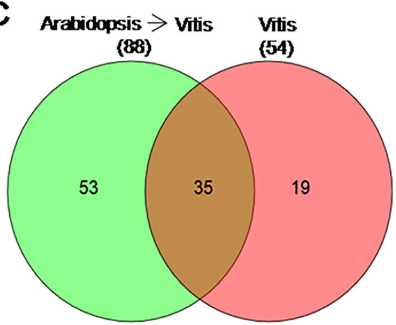

D

	Motif	Logo	E-value	Frequency in the predicted *VlbZIP30* induced genes (%)		Frequency in the genome (%)
				In 35 genes	In 196 genes	
1	MCACGTGK		1.9e-009	100.0	77.4	59.0
2	RAGAGARA		2.4e-007	91.4	74.2	63.9
3	CACSTC		3.5e-004	100.0	85.5	87.9

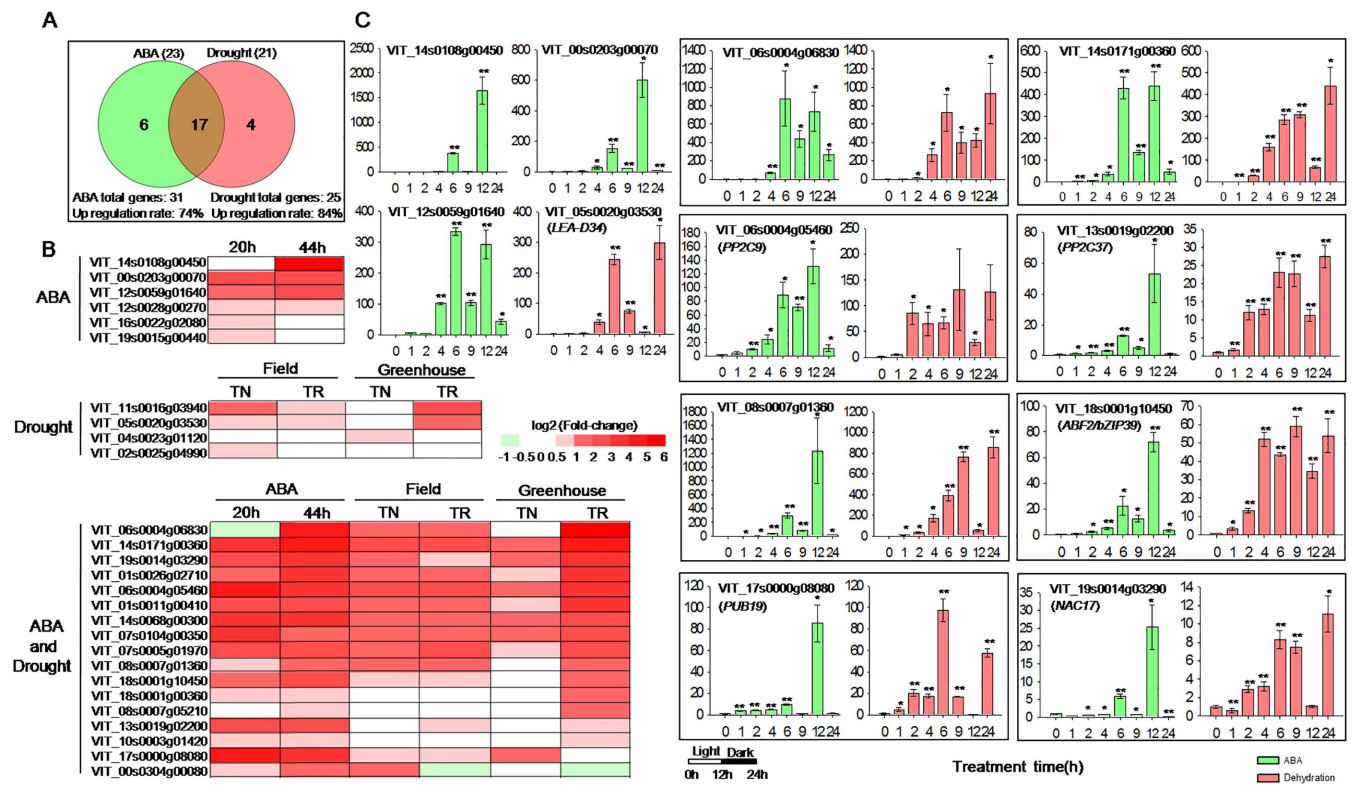
A
ABA (23)
Drought (21)
6
17
4
ABA total genes: 31
Drought total genes: 25
Up regulation rate: 74%
Up regulation rate: 84%
B
20h
44h
ABA
VIT_14s0108g00450
VIT_00s0203g00070
VIT_12s0059g01640
VIT_12s0028g00270
VIT_16s0022g02080
VIT_19s0015g00440
Field
Greenhouse
TN
TR
TN
TR
Drought
VIT_11s0016g03940
VIT_05s0020g03530
VIT_04s0023g01120
VIT_02s0025g04990
log2 (Fold-change)
-1 -0.5 0 0.5 1 2 3 4 5 6
ABA
Field
Greenhouse
20h
44h
TN
TR
TN
TR
ABA and Drought
VIT_06s0004g06830
VIT_14s0171g00360
VIT_19s0014g03290
VIT_01s0026g02710
VIT_06s0004g05460
VIT_01s0011g00410
VIT_14s0068g00300
VIT_07s0104g00350
VIT_07s0005g01970
VIT_08s0007g01360
VIT_18s0001g10450
VIT_18s0001g00360
VIT_08s0007g05210
VIT_13s0019g02200
VIT_10s0003g01420
VIT_17s0000g08080
VIT_00s0304g00080
C
VIT_14s0108g00450
VIT_00s0203g00070
VIT_12s0059g01640
VIT_05s0020g03530
(LEA-D34)
VIT_06s0004g06830
VIT_14s0171g00360
VIT_06s0004g05460
(PP2C9)
VIT_13s0019g02200
(PP2C37)
VIT_08s0007g01360
VIT_18s0001g10450
(ABF2/bZIP39)
VIT_17s0000g08080
(PUB19)
VIT_19s0014g03290
(NAC17)
0 1 2 4 6 9 12 24
Light Dark
0h 12h 24h
Treatment time(h)
ABA
Dehydration

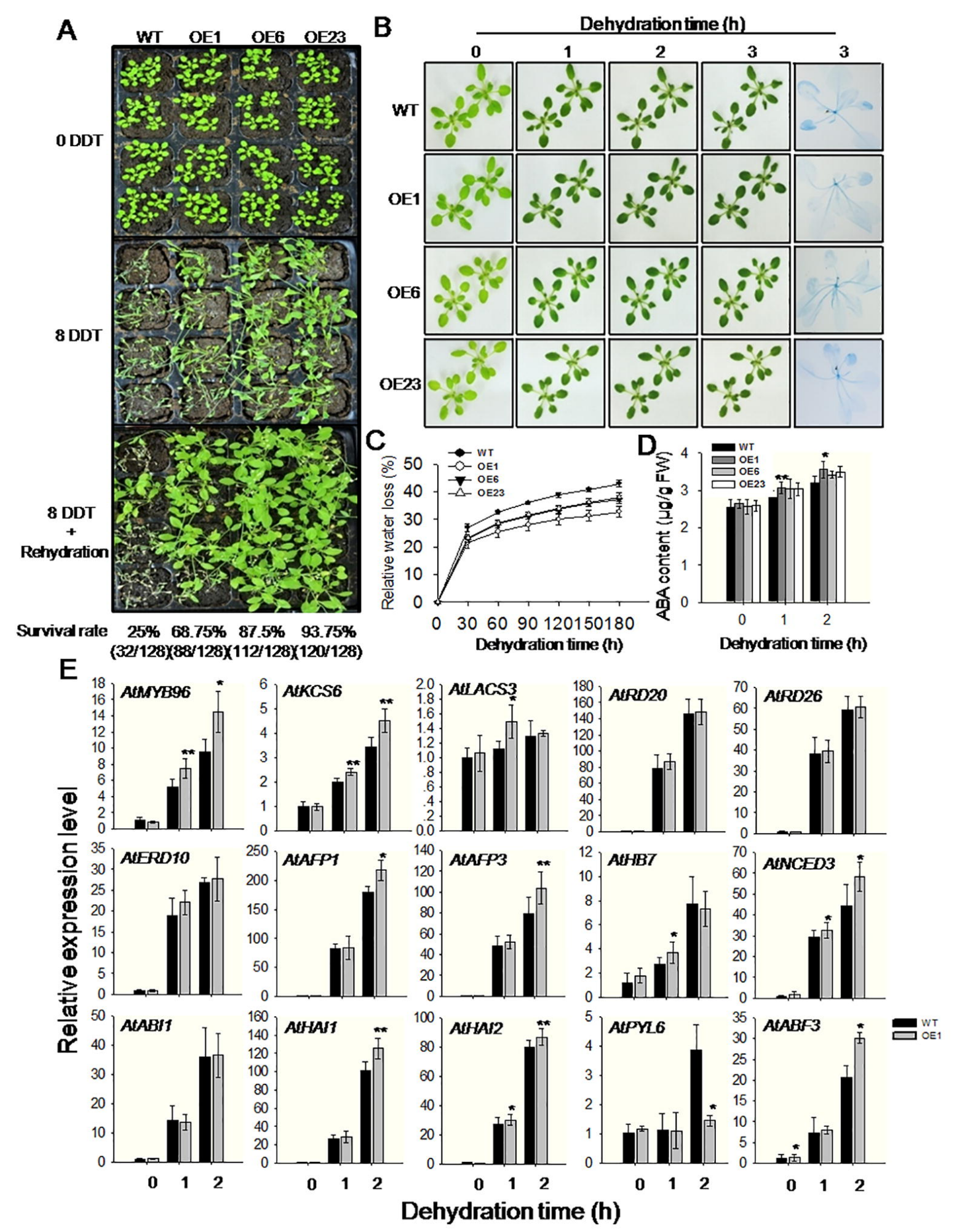
A
WT
OE1
OE6
OE23
0 DDT
8 DDT
8 DDT + Rehydration
Survival rate 25% 68.75% 87.5% 93.75%
(32/128)(88/128)(112/128)(120/128)
B
Dehydration time (h)
0
1
2
3
3
WT
OE1
OE6
OE23
C
Relative water loss (%)
Dehydration time (h)
D
ABA content (μg/g FW)
Dehydration time (h)
E
Relative expression level
AtMYB96
AtKCS6
AtLACS3
AtRD20
AtRD26
AtERD10
AtAFP1
AtAFP3
AtHB7
AtNCED3
AtABI1
AtHAI1
AtHAI2
AtPYL6
AtABF3
Dehydration time (h)